

# Thermodynamics of small Fermi systems: quantum statistical fluctuations

P. Leboeuf and A. G. Monastra

*Laboratoire de Physique Théorique et Modèles Statistiques \*, Bât. 100,  
91405 Orsay Cedex, France*

We investigate the probability distribution of the quantum fluctuations of thermodynamic functions of finite, ballistic, phase-coherent Fermi gases. Depending on the chaotic or integrable nature of the underlying classical dynamics, on the thermodynamic function considered, and on temperature, we find that the probability distributions are dominated either (i) by the local fluctuations of the single-particle spectrum on the scale of the mean level spacing, or (ii) by the long-range modulations of that spectrum produced by the short periodic orbits. In case (i) the probability distributions are computed using the appropriate local universality class, uncorrelated levels for integrable systems and random matrix theory for chaotic ones. In case (ii) all the moments of the distributions can be explicitly computed in terms of periodic orbit theory, and are system-dependent, non-universal, functions. The dependence on temperature and number of particles of the fluctuations is explicitly computed in all cases, and the different relevant energy scales are displayed.

## I. INTRODUCTION

Self-consistent theories which admit almost independent motion of quasiparticles and give rise to Fermi gases constitute a basic tool to describe fermionic many-body systems. Well known examples are independent-particle models in nuclear physics, quantum dots and wires in condensed matter physics and, within a mean-field theory for the valence electrons, the jellium model for the electronic properties of metals and of simple alkali metal clusters. One of the most spectacular predictions of mean-field theories is the occurrence of shell effects in the energy of the fermion gas as a function of the number of particles, that leads to magic numbers and deformations in nuclei and metallic particles [1,2]. The shell and super-shell structures are quantum fluctuations that describe the bunching of the single-particle energy levels with respect to their average behavior. From a semiclassical point of view [3,4], the bunching of the energy levels is interpreted as a modulation produced by the classical periodic orbits.

Similar quantum fluctuations are present in all the equilibrium thermodynamic functions describing the many-body system. As we will see in detail in the following, there are two main features of the single-particle spectrum that influence the thermodynamic quantum fluctuations of a Fermi gas. On the one hand, the spectral fluctuations on local scales, i.e. in the range of the mean level spacing  $\delta$  between single-particle energy levels. These local fluctuations are universal, and the universality class depends on the nature of the single-particle dynamics [5,6]. There are two main classes, corresponding to regular and irregular (fully chaotic) motion, respectively (with subclasses in the latter case depending on the presence or not of time reversal symmetry). The local statistics of regular systems are described by a set of uncorrelated levels, while the chaotic ones by random matrix ensembles.

The second ingredient that strongly influences the thermodynamic fluctuations are the shell effects, i.e. the long range modulations of the spectrum produced by the short periodic orbits. These occur on a scale  $E_c$  related to the inverse time of flight across the system, with typically  $E_c \gg \delta$ . Contrary to the local fluctuations, the long-range modulations are system-dependent, since the short orbits are. The amplitude of this effect depends on the nature of the dynamics. If the classical motion is regular, symmetries are present, periodic orbits come in degenerate families, and shell effects are important. On the contrary, if the corresponding classical motion is chaotic, the periodic orbits are isolated and the long-range modulations will have, compared to the regular case, a smaller amplitude. Different aspects of both quantum phenomena, namely the universality of the single-particle fluctuations on a scale  $\delta$  and the appearance of long-range shell effects on scales  $E_c$ , and their influence in the thermodynamics of Fermi gases, have been considered in nuclear and atomic physics, and in different condensed-matter systems (see for example Refs. [1,2,7,8]). In most cases the interest concentrated on particular systems, or in the study of mean properties.

Our main goal is, within a Fermi gas approximation, to provide a statistical analysis of the quantum fluctuations of the different thermodynamic functions, like for example of the total energy of the gas, the entropy, etc, and to explicitly compute their probability distribution function. Special attention is devoted to the temperature dependence and to the typical magnitude of the fluctuations. Other aspects, like the autocorrelation functions and the connexion between the fluctuations of the gas and those of the single-particle levels at Fermi energy, are also investigated. We

---

\*Unité de recherche de l'Université de Paris XI associée au CNRS

concentrate in the fluctuations of equilibrium properties of *ballistic* Fermi systems (i.e. with no disorder present in the potential) whose mean-field single particle motion is either regular or fully chaotic. Schematically we have in mind a mean-field potential which is almost flat in the interior and rises at the surface, like the Woods-Saxon potential in nuclear physics, or the static homogeneous potential produced by the ionic background in the jellium model. Under these conditions, and in particular in the extreme case of a sharp boundary, the nature of the classical dynamics is determined by the shape of the cavity and by the external fields acting on the system. We will ignore physical effects related to the spin degree of freedom, and we will moreover assume that the inelastic processes can be ignored, namely the coherence length of the fermions is much larger than the system size.

The picture that emerges from our analysis is very rich. The quantum thermodynamic fluctuations can be either dominated by the local universal or by the long-range system-specific fluctuations of the single particle spectrum. Among these two possibilities, the prevailing aspect depends on the quantity considered, on the nature of the underlying classical dynamics, and on temperature. When the fluctuations are dominated by the local fluctuations, the corresponding thermodynamic probability distributions are universal. When conveniently normalized, they only depend on the temperature and the quantity considered, but not on any specific property of the system (aside the regular or chaotic nature of the single-particle motion). The universality of the thermodynamic fluctuations follows the classification of the local fluctuations given above: one universality class for systems whose classical single-particle dynamics is regular, another for those with a chaotic dynamics (with subclasses depending on the presence or not of time reversal symmetry). Universal fluctuations are observed, for some thermodynamic functions, at temperatures much smaller than  $E_c$ . Examples are the fluctuations of the number of particles for systems with fixed chemical potential when the underlying classical dynamics is chaotic, and those of the entropy and the specific heat for regular and chaotic motion. The corresponding probability distributions are found to be, in general, non-Gaussian. For temperatures of order  $\delta$  their shape is very sensitive to temperature variations, but they always remain in the corresponding universality class. When temperatures of order  $E_c$  are reached, the universality is lost. At those temperatures the short orbits become dominant, producing system-dependent effects. The moments of the distributions can then be computed from periodic orbit theory, as described below. At still higher temperatures the fluctuations are exponentially suppressed.

In contrast to the first type described above, sometimes the thermodynamic fluctuations are dominated by the long range modulations of the single-particle spectrum produced by the short periodic orbits. Due to the system specific nature of the short orbits, the corresponding probability distributions are non-universal, non-Gaussian functions. We have obtained explicit convergent expressions to compute all the moments for this type of fluctuations in terms of periodic orbits. Interference effects between repetitions of the orbits produce, in particular, non-vanishing odd moments and lead to asymmetric distributions. The fluctuations of all the thermodynamic functions are of this type for temperatures of order  $E_c$  or higher. However, some thermodynamic functions have non-universal fluctuations *at any temperature*. Examples of the latter behavior are the fluctuations of the total energy of the gas, the response of the system when an external parameter is varied and, only in the case of a regular single-particle dynamics, the fluctuations of the number of particles for systems with fixed chemical potential. Due to the dominance of the long range modulations, the probability distributions are relatively insensitive to temperature variations up to temperatures of order  $E_c$ . At temperatures higher than  $E_c$  the typical size of the fluctuations decay exponentially. Finally, the autocorrelation functions in this case present long range order.

As a general rule, but with exceptions depending on the quantity and on the temperature considered, clear signatures of the regular or chaotic nature of the dynamics are found in the fluctuations. For example, their typical size is in general much larger in integrable systems compared to chaotic ones. The relative amplifying factor is found to be some growing function of the adimensional parameter  $g = E_c/\delta$ . Besides, and irrespective of the nature of the dynamics, the fluctuations of the gas are always much larger than the corresponding fluctuations of the single-particle energy levels at Fermi energy. Their relation is also expressed in terms of  $g$ .

The paper is organized as follows. Section II contains the basic definitions concerning the thermodynamics of a Fermi gas. An arbitrary thermodynamic function is decomposed into a smooth plus an oscillatory part. The smooth part describes the usual thermodynamics of the gas (bulk properties), while the oscillatory part are the quantum finite-size fluctuations. The latter are expressed in terms of the periodic orbits of the classical motion associated with the corresponding single-particle dynamics. The validity of this approximation and the main energy scales involved in the problem are also introduced. In Section III the variance of the thermodynamic functions is written in terms of the spectral form factor, i.e. the Fourier transform of the single-particle spectral two-point correlation function (Eq.(29)). This connexion allows to make a qualitative analysis of the behavior of the moments of the probability distribution of the different functions and for the different kinds of classical motions. The second moment is explicitly computed in Section IV using a schematic approximation for the short-time dynamics that provides simple but qualitatively useful expressions. The dependence on particle number and on temperature is explicitly considered. The complete characterization of the probability distribution of the fluctuations is included in Section V. The moments are explicitly computed for quantities whose distribution is dominated, by the short orbits. On the contrary, local uncorrelated levels

and random matrix fluctuations are used to compute the distribution of universal functions (at low temperatures). Similar arguments are exploited in Section VI to compute the autocorrelation of the thermodynamic functions as a function of the different parameters. The application of our general results to different systems, like the atomic nuclei, mesoscopic quantum dots and metallic clusters is briefly discussed in Section VII. This section contains also a discussion on the relation between the fluctuations of the gas and those of the individual single-particle energy levels. Our final remarks are included in Section VIII. All over the paper we compare some of the results with numerical simulations of Fermi gases contained in regular and chaotic cavities.

## II. GENERAL SETTING

### A. Basic equations

When the chemical potential  $\mu$  is fixed the thermodynamic behavior of a non-interacting Fermi gas is described by the grand potential

$$\Omega(x, \mu, T) = -k_B T \int dE \rho(E, x) \log[1 + e^{(\mu-E)/k_B T}] , \quad (1)$$

where

$$\rho(E, x) = g_s \sum_j \delta[E - E_j(x)] \quad (2)$$

is the density of states of the single-particle energy levels  $E_j(x)$ . The parameter  $x$  denotes the dependence on some external parameter,  $T$  is the temperature, and  $k_B$  is Boltzmann's constant. The prefactor  $g_s = 2$  when spin degeneracy exists. For simplicity we will from now on omit it, but it can be easily restored in the final results.

When the number of particles  $N$  in the gas is fixed, the energy of the system is

$$U(x, N, T) = \int dE E \rho(E, x) f(E, \mu, T) , \quad (3)$$

where  $\mu$  is determined from the equation

$$N = \int dE \rho(E, x) f(E, \mu, T) , \quad (4)$$

and  $f$  is the Fermi function

$$f(E, \mu, T) = \frac{1}{1 + e^{(E-\mu)/k_B T}} . \quad (5)$$

Knowing these two thermodynamic potentials, other thermodynamic functions are directly obtained by differentiation. For example, in the grand canonical formalism the expectation value of the number of particles in the system is

$$\mathcal{N}(x, \mu, T) = - \left. \frac{\partial \Omega}{\partial \mu} \right|_{x, T} . \quad (6)$$

Another important thermodynamic quantity is the reaction of the system to a variation of the external parameter  $x$ , characterized by the response function (here in the grand canonical formalism)

$$R(x, \mu, T) = - \left. \frac{\partial \Omega}{\partial x} \right|_{\mu, T} . \quad (7)$$

The physical interpretation of  $R$  depends on the sample geometry and on the nature of the parameter  $x$ .  $R$  is the orbital magnetization when  $x$  is a magnetic field, a persistent current when the sample geometry is annular and  $x$  is an Aharonov-Bohm flux, or a force (pressure) when  $x$  controls the shape of the confining potential (like when deforming a nucleus for example; at equilibrium, the nucleus shape is defined by  $R = 0$ ). Finally, we will also consider the entropy

$$S(x, \mu, T) = - \left. \frac{\partial \Omega}{\partial T} \right|_{\mu, x} \quad (8)$$

from which, in particular, the many-body level density may be computed by exponentiation, and the specific heat (in the canonical ensemble)

$$c_x = \left. \frac{\partial U}{\partial T} \right|_{N, x} . \quad (9)$$

The case of the susceptibility, i.e. the variation of the response function (the second derivative of the grand potential)

$$\chi(x, \mu, T) = \left. \frac{\partial R}{\partial x} \right|_{\mu, T} = - \left. \frac{\partial^2 \Omega}{\partial x^2} \right|_{\mu, T} \quad (10)$$

is a more subtle problem and will not be considered here in detail.

Assuming the single-particle spectrum Eq. (2) known for any  $x$ , the integration in Eq.(1) is straightforward. It leads, by differentiation, to sums over the single-particle energy levels whose structure depends on the quantity considered. As the temperature is lowered the Fermi factor  $f(E, \mu, T)$  involved in the sums tends to the Heaviside step function, which restricts the sums to the single-particle energy levels satisfying the condition  $E_j(x) \leq \mu$ . In this limit the grand potential is closely related to the ground state energy of the Fermi gas (it is the sum of the single particle energy levels measured with respect to the Fermi energy),  $\mathcal{N}$  is the number of occupied single-particle levels, and the response of the system is the sum up to the Fermi energy of the single-particle contributions  $\partial E_j / \partial x$ . They all involve the ensemble of particles of the Fermi gas. In contrast, other quantities, like the entropy and the specific heat, vanish at zero temperature.

## B. Semiclassical approximation

We now express the thermodynamic functions in terms of classical quantities related to the single-particle dynamics (cf Ref. [9] for a good introduction). The density of states in Eq.(1) is written as a sum of smooth plus oscillatory terms

$$\rho(E, x) = \bar{\rho}(E, x) + \tilde{\rho}(E, x) . \quad (11)$$

This approximation is valid in the semiclassical regime  $\mu \gg \delta$  where the typical wavelength of the fermions at energy  $\mu$  is much smaller than the system size, and fails at the bottom of the spectrum. The first, smooth term  $\bar{\rho}$  corresponds to the bulk contribution. For example, when the gas is simply contained in a finite volume  $V$  of space having an arbitrary shape, and the single-particle levels are filled up to a Fermi energy  $E_F$  with particles of mass  $m$ , the average number of occupied levels is, to leading order

$$\bar{\mathcal{N}} = \frac{4V}{3\sqrt{\pi}} \left( \frac{m}{2\pi\hbar^2} \right)^{3/2} E_F^{3/2} , \quad (12)$$

while the mean level density  $\bar{\rho}$  and corresponding mean level spacing  $\delta$  between single-particle states are

$$\bar{\rho} = \delta^{-1} = \frac{2V}{\sqrt{\pi}} \left( \frac{m}{2\pi\hbar^2} \right)^{3/2} E_F^{1/2} . \quad (13)$$

The substitution in Eqs.(1) and (3) of the density of states by its average behavior, Eq.(13), gives rise to the smooth, bulk classical expressions for the thermodynamics of the gas [10]. In finite fermionic systems, like the atomic nucleus or a metallic particle, the smooth part coming from the single-particle potential is of no use, and is rather computed in a self-consistent manner from the original many-body problem [11].

The most relevant contribution to the many-body problem is the fluctuating part, which is of quantum mechanical origin, and describes the discreteness of the single-particle spectrum. It is given by a sum over the classical periodic orbits [3,12]. To leading order in an  $\hbar$ -expansion

$$\tilde{\rho}(E, x) = 2 \sum_p \sum_{r=1}^{\infty} A_{p,r}(E, x) \cos [rS_p(E, x)/\hbar + \nu_{p,r}] . \quad (14)$$

The sum is over all the primitive periodic orbits  $p$  (and its repetitions  $r$ ). The orbits are characterized by their action  $S_p$ , period  $\tau_p = dS_p/dE$ , stability amplitude  $A_{p,r}$ , and Maslov index  $\nu_{p,r}$ .

Explicit expressions for  $A_{p,r}$  are available. Their functional form depends on the nature of the dynamics. For a  $d$ -dimensional integrable system, where action-angle variables exist, the periodic orbits are organized on resonant tori, i.e.  $d$ -dimensional manifolds having the topology of a torus with commensurate frequencies. If  $I_j$  are the action variables, then the frequencies are  $\omega_j = \partial H/\partial I_j = 2\pi m_j/\tau_p$ , where the  $m_j$  are integers that label the periodic orbits (that we abbreviate in the unique index  $p$ ). When the  $\{m_j\}$  have no common divisor they label a primitive periodic orbit, otherwise it is a repetition. The  $A_p$ 's take in this case the form [13]

$$A_p^2 = \frac{(2\pi)^{d-1}}{\hbar^{d+1} \tau_p^d \left| \det\{\partial\omega_j/\partial I_k\}_p \sum_j \omega_j \cdot \partial I_j/\partial \tau_p \right|}. \quad (15)$$

The repetitions do not appear explicitly, and are considered as primitive periodic orbits. Instead, in chaotic system the amplitudes are [12]

$$A_{p,r} = \frac{\tau_p}{h\sqrt{|\det(M_p^r - I)|}}. \quad (16)$$

Here  $I$  is the identity matrix and  $M_p$  the monodromy matrix obtained from the linearization of the equations of motion in the vicinity of the corresponding primitive periodic orbit. In both cases the Maslov indices  $\nu_{p,r}$  are constant phase factors (locally) independent of the energy and of the external parameter.

Eq.(14) is inserted in Eq.(1) to compute the oscillatory part of the grand potential. To leading order in  $\hbar$  and for low temperatures ( $k_B T \ll \mu$ , degenerate gas approximation)

$$\tilde{\Omega}(x, \mu, T) \approx 2\hbar^2 \sum_p \sum_{r=1}^{\infty} \frac{A_{p,r} \kappa_T(r \tau_p)}{r^2 \tau_p^2} \cos(rS_p/\hbar + \nu_{p,r}). \quad (17)$$

The classical functions entering in this expressions are evaluated at  $E = \mu$ , and they all depend on the external parameter  $x$ . The temperature introduces the prefactor  $\kappa_T(\tau)$ , which acts as an exponential cut off for the long orbits [1]

$$\kappa_T(\tau) = \frac{\tau/\tau_T}{\sinh(\tau/\tau_T)}, \quad \tau_T = h/(2\pi^2 k_B T). \quad (18)$$

For temperatures such that  $\tau_T \ll \tau_{min}$ , with  $\tau_{min}$  the period of the shortest periodic orbit, the quantum fluctuations are washed out and only the smooth behavior given by  $\bar{\rho}$  survives.

Similarly we may analyze the energy of the gas at a fixed number of particles. The smooth part of  $U$  differs from that of  $\Omega$ , but to leading order in a semiclassical expansion we find that their fluctuating parts coincide.  $\tilde{U}$  is thus given by an equation identical to Eq. (17), with  $\mu$  not a continuous variable but now a function of  $N$ ,  $x$  and  $T$  determined by Eq.(4) but where  $\bar{\rho}$  is used instead of  $\rho$ ,

$$\tilde{U}(x, N, T) = \tilde{\Omega}(x, \mu(x, N, T), T). \quad (19)$$

The prefactor  $A_{p,r} \kappa_T(r \tau_p)/\tau_p^2$  in Eq. (17) varies smoothly with the external parameter, the chemical potential, or temperature. The main contribution to the oscillatory behavior of the grand potential comes in fact from the variations of the phase factor  $rS_p(x, \mu)/\hbar$  with respect to  $x$  and  $\mu$ . When differentiating Eq. (17) or Eq. (19) to compute the fluctuating part of other thermodynamic quantities according to Eqs. (6)-(10) we only keep, to first order in a semiclassical expansion in  $\hbar$ , the terms coming from the variations of the phase factor. In this approximation, the fluctuating part of all the thermodynamic quantities considered has the same structure, and can be written in a compact form as

$$\tilde{\Phi}(x, \mu, T) = 2 \mathcal{C} \sum_p \sum_{r=1}^{\infty} \mathcal{A}_{p,r}(x, \mu, T) \cos[rS_p(x, \mu)/\hbar + \nu_{p,r}]. \quad (20)$$

The constant coefficient  $\mathcal{C}$  includes all the terms not depending on the periodic orbits. This coefficient, as well as the orbit-dependent prefactor  $\mathcal{A}_{p,r}$  computed in the leading semiclassical approximation, are given for some of the thermodynamic functions in Table I. When necessary, the sine functions have been systematically transform into

cosines by subtracting a  $\pi/2$  to each Maslov index. The prime in  $\kappa'_T$  denotes the derivative of  $\kappa_T$  with respect to temperature,  $\kappa'_T = \partial\kappa_T/\partial T$ , while

$$Q_p = \left. \frac{\partial S_p}{\partial x} \right|_{\mu} . \quad (21)$$

Eq.(20), together with Table I, are the basic expressions on which the study of the probability distributions of the fluctuations is based on. The knowledge of the periodic orbits (or at least of those satisfying, at finite temperature,  $\tau_p \lesssim \tau_T$ ) allows to explicitly compute, using Eq.(20), the quantum oscillatory contributions to  $\Phi$ . We are interested, however, in a statistical analysis valid for a generic system rather than in an explicit computation for a particular one.

	$\mathcal{C}$	$\mathcal{A}_{p,r}$	$F(\tau)$
$\tilde{U}$	$\hbar^2$	$A_{p,r} \kappa_T(r\tau_p)/r^2\tau_p^2$	$\kappa_T^2(\tau)$
$\tilde{N}$	$\hbar$	$A_{p,r} \kappa_T(r\tau_p)/r\tau_p$	$\tau^2 \kappa_T^2(\tau)$
$\tilde{R}$	$\hbar$	$A_{p,r} Q_p \kappa_T(r\tau_p)/r\tau_p^2$	$Q^2(\tau) \kappa_T^2(\tau)$
$\tilde{S}$	$\hbar^2$	$A_{p,r} \kappa'_T(r\tau_p)/r^2\tau_p^2$	$\kappa_T'^2(\tau)$

**Table I:** the coefficient  $\mathcal{C}$  and prefactor  $\mathcal{A}_{p,r}$  of Eq.(20) for different thermodynamic functions. See the text for details. In the third column is listed the function  $F(\tau)$  appearing in Eq. (29).

As  $T \rightarrow 0$  the sum (20) over periodic orbits is in general divergent. For instance, in fully chaotic systems it diverges for temperatures  $T \lesssim \hbar\xi/2\pi k_B$  (where  $\xi$  is the Lyapounov exponent), and converges otherwise. Using resummation techniques finite sums may be obtained, as was done for example for the magnetic susceptibility of two-dimensional billiards in [14]. However, we will not need to proceed along these lines since, as we will see, *the moments* of the thermodynamic quantities based on these sums are, in some cases, *convergent*. In the cases where they don't, the distributions will be directly determined from the local universal fluctuations.

### C. Averages, energy and parameter scales

There are several different energy scales that are relevant when considering the quantum thermodynamic fluctuations. The smallest energy scale in the problem is the single-particle mean level spacing  $\delta = \bar{\rho}^{-1}$  at the Fermi energy  $\mu$  (since  $k_B T \ll \mu$ , we don't make in this qualitative considerations the difference between the chemical potential and the Fermi energy). The time scale associated to this energy is the Heisenberg time

$$\tau_H = h/\delta . \quad (22)$$

The largest energy scale is the Fermi energy  $E_F$ , or chemical potential  $\mu$ . The third relevant energy scale has a simple semiclassical origin. According to Eq. (20), locally each periodic orbit  $p$  produces a periodic modulation (in energy) of wavelength  $\lambda_p \sim h/\tau_p(\mu)$ . Since there are orbits of arbitrary long period,  $\lambda_p$  can be arbitrarily small. There is on the contrary an upper bound to  $\lambda_p$  determined by the period  $\tau_{min}$  of the shortest periodic orbit (at  $E = \mu$ ). The corresponding energy scale is

$$E_c = h/\tau_{min} . \quad (23)$$

This is the largest scale in which long-range modulations of the single-particle spectrum occur, and fixes the size of the shell structures at  $E = E_F$ . The ratio of  $E_c$  to  $\delta$  is another important parameter

$$g = \tau_H/\tau_{min} = E_c/\delta . \quad (24)$$

The energy  $E_c$  and the adimensional parameter  $g$  are, in some respects, the analog for ballistic systems of the Thouless energy and the adimensional conductance defined in diffusive systems, respectively [15,8]. Its physical meaning in ballistic systems is clear from Eq. (24). It is the number of single-particle states contained in the last shell, which is of size  $E_c$ . It is therefore a measure of the collective effect of the modulations produced by the shell contributions, a “shell-strength” parameter.

Assuming the typical system-size is  $L$ , it is useful to display the different energy scales  $\delta$ ,  $E_c$ , and  $\mu$  in terms of the typical number of the De Broglie wavelengths the system can accommodate at Fermi energy,  $k_F L$ , where  $k_F$  is the Fermi wavevector. These estimates are based on the generalization of Eqs. (12) and (13) to a  $d$ -dimensional cavity. On the one hand we have  $g = E_c/\delta \propto (k_F L)^{d-1}$ . Moreover,  $\mu/E_c = k_F L/2\pi$ . Thus, in the semiclassical regime  $k_F L \gg 1$  where our description applies, the parameter  $g$  is large, and the different energy scales are well separated,  $\delta \ll E_c \ll \mu$ .

The fourth relevant energy scale is the temperature. Eq. (20) is valid in the limit  $k_B T \ll \mu$  of a strongly degenerate gas, which is the relevant limit for most physical applications. Notice the large coefficient  $2\pi^2 \approx 20$  involved in the parameter  $\tau_T$  in Eq.(18), as compared to Eqs. (22) and (23). This large coefficient cannot be ignored, and therefore the relevant thermal energy to be compared with the quantum scales  $E_c$  and  $\delta$  is  $2\pi^2 k_B T$ .

The fluctuating part of a given thermodynamic function  $\tilde{\Phi}$  shows, as a function of the chemical potential  $\mu$ , oscillations described by Eq. (20). The statistical properties of  $\tilde{\Phi}$ , and in particular its probability distribution, will be computed in a given interval of size  $\Delta\mu$  around  $\mu$ . This interval must satisfy two conditions. It must be sufficiently small in order that all the classical properties of the system remain almost constant. This is fulfilled if  $\Delta\mu \ll \mu$ . Moreover, it must contain a sufficiently large number of oscillations to guarantee the convergence of the statistics. As stated previously the largest scale associated to the oscillations is  $E_c$ . Then clearly we must have  $\Delta\mu \gg E_c$ . In the semiclassical regime the hierarchical ordering between the different scales is therefore

$$\delta \ll E_c \ll \Delta\mu \ll \mu .$$

Since  $\mu/E_c \propto k_F L$ , a typical scale for the smoothing energy window is  $\Delta\mu/E_c \propto (k_F L)^{1/2}$ . We thus define the energy average of a certain oscillating function as

$$\langle f(\mu) \rangle_\mu \equiv \frac{1}{\Delta\mu} \int_{\mu-\Delta\mu/2}^{\mu+\Delta\mu/2} f(\mu') d\mu' . \quad (25)$$

In a similar way a parameter average is defined as

$$\langle f(x) \rangle_x \equiv \frac{1}{\Delta x} \int_{x-\Delta x/2}^{x+\Delta x/2} f(x') dx' , \quad (26)$$

where  $\Delta x$  is defined by similar arguments as  $\Delta\mu$ . As in the energy average, the classical properties must not significantly change in the interval  $\Delta x$ , but it must contain several oscillations to make a statistical analysis appropriate. The largest scale associated to these parameter oscillations is again related to the shortest orbit, and given by  $h/Q_{min}$ .

We finally note that if all these conditions are satisfied both the energy and parameter averages gives the same result, and consequently commute.

### III. QUALITATIVE ANALYSIS OF THE DISTRIBUTIONS

By definition, the average value of the fluctuating part  $\tilde{\Phi}$  is zero. Aside the average value, the variance is the more basic aspect of the probability distribution of the fluctuations. It provides the typical size of the oscillations, and can easily be compared with experiments. We will now compute a general expression for the second moment that allows to make a qualitative analysis of the distribution of the different thermodynamic quantities. Similar arguments for the higher moments lead to similar conclusions.

From Eq. (20) the square of  $\tilde{\Phi}$  is expressed as a double sum over the periodic orbits involving the product of two cosines. The latter may be expressed as one half the sum of the cosine of the sum and that of the difference of the actions. The average over the term containing the sum of the actions vanishes, due to its rapid oscillations on a scale  $\Delta\mu$ . Therefore

$$\langle \tilde{\Phi}^2 \rangle = 2 \mathcal{C}^2 \left\langle \sum_{p,p'} \mathcal{A}_p \mathcal{A}_{p'} \cos \left( \frac{S_p - S_{p'}}{\hbar} \right) \right\rangle_{\mu,x} . \quad (27)$$

To simplify the notation we have momentarily considered the repetitions of a primitive orbit as a different primitive periodic orbit, and have included the Maslov indices in the definition of the action. Ordering the orbits by their period, and taking into account the restrictions imposed by the averaging procedure, we can relate the variance Eq. (27) to the semiclassical definition of the form factor  $K(\tau)$  (i.e., the Fourier transform of the two-point correlation function  $\langle \tilde{\rho}(\mu + \epsilon/2) \tilde{\rho}(\mu - \epsilon/2) \rangle_\mu$  with respect to  $\epsilon$ ), expressed as [16]

$$K(\tau) = h^2 \left\langle \sum_{p,p'} A_p A_{p'} \cos \left( \frac{S_p - S_{p'}}{\hbar} \right) \delta \left[ \tau - \frac{(\tau_p + \tau_{p'})}{2} \right] \right\rangle_{\mu,x} . \quad (28)$$

The form factor defined in Eq. (28) has units of time. When expressed in terms of  $K(\tau)$ , the variance of the quantum thermodynamic fluctuations considered above takes the simple form

$$\langle \tilde{\Phi}^2 \rangle = \frac{\mathcal{C}^2}{2\pi^2 \hbar^2} \int_0^\infty \frac{d\tau}{\tau^4} K(\tau) F(\tau) , \quad (29)$$

where  $F(\tau)$  depends on the thermodynamic function considered (cf Table I). Analogous expressions connecting the variance of different quantities like the persistent current or the conductance fluctuations have been obtained when describing disordered metals [17]. In the latter case, the form factor for times  $\tau \ll \tau_H$  is closely related to the classical return probability for a diffusive particle.

To obtain Eq.(29) we made use of the fact that the orbits giving a non-zero contribution to (27) have similar actions (unless their average will be zero). This implies that their period is also similar, and can be considered to be the same in the prefactor (but not in the argument of the oscillating part). Similar arguments apply to the  $Q_p$ 's. It can be shown by arguments invoking the stationarity of the form factor under variations of the external parameter  $x$  that the contributing orbits have very similar derivatives  $Q_p$ . The factor  $Q^2(\tau)$  entering the variance of the response function has a statistical meaning. When replacing the double sum in Eq. (27) by an integral over the period  $\tau$ , among all the periodic orbits  $p$  of period between  $\tau$  and  $\tau + d\tau$  we consider the distribution of the derivatives (21). Then  $Q^2(\tau)$  is the second moment of that distribution. The expression (29) for the response function therefore neglects the non-statistical behavior of the short orbits.

By definition, the form factor (28) is system dependent. But general statistical statements, depending only on the nature of the underlying classical dynamics, have been conjectured for ballistic systems. When the classical dynamics is integrable, the quantum energy levels are believed to behave as an uncorrelated sequence [6]. This implies no  $\tau$ -dependence of the form factor,

$$K_{int}(\tau) = \tau_H , \quad (30)$$

where  $\tau_H$  was defined in Eq. (22). The situation is different for fully chaotic systems, where it has been conjectured that the fluctuations are described by the corresponding ensembles of random matrix theory [5,18]. For the form factor it gives

$$K_{rmt}(\tau) = \begin{cases} \left[ 2\tau - \tau \log \left( 1 + \frac{2\tau}{\tau_H} \right) \right] \Theta(\tau_H - \tau) + \left[ 2\tau_H - \tau \log \left( \frac{2\tau + \tau_H}{2\tau - \tau_H} \right) \right] \Theta(\tau - \tau_H) & \beta = 1 \\ \tau \Theta(\tau_H - \tau) + \tau_H \Theta(\tau - \tau_H) & \beta = 2 . \end{cases} \quad (31)$$

where  $\beta = 1$  (2) for systems with (without) time-reversal symmetry (since we are neglecting the role of spin we do not include the symplectic symmetry). For short times  $\tau \ll \tau_H$  this function behaves as

$$K_{rmt}(\tau) = \frac{2}{\beta} \tau . \quad (32)$$

Aside the form factor, to compute the variance of the response function information about the  $Q_p$ 's is required. For chaotic systems numerical evidence as well as general considerations suggest a Gaussian distribution, with zero average (if the area of the cavity is preserved when  $x$  varies) and variance proportional to the period  $\tau$  [19]. Then  $Q^2(\tau) \approx \alpha\tau$ , where  $\alpha$  is some system-dependent constant which corresponds to a classical diffusion coefficient [20]. In the integrable case no universal distribution exists for the  $Q_p$ 's, but explicit calculations for some integrable systems as well as general heuristic arguments indicate that the second moment is proportional to  $\tau^2$  [21]. In summary

$$Q^2(\tau) = \begin{cases} \alpha\tau & \text{chaotic ,} \\ \omega\tau^2 & \text{integrable .} \end{cases} \quad (33)$$



For short times, Eqs. (30) and (32) are good approximations in real systems in the regime  $\tau_{min} \ll \tau \ll \tau_H$ . Their semiclassical origin is related to the statistical behavior of the long classical periodic orbits [22,16].

For times of the order of  $\tau_{min}$  no statistical universal behavior of the form factor exists, and Eq. (30) and (32) do not provide a good description. For such times the off-diagonal contributions in Eq. (28) are eliminated by the averaging procedure, and the behavior of  $K(\tau)$  is described by a series of delta peaks at  $\tau = \tau_p$  obtained from the diagonal terms  $p = p'$  in the double sum

$$K(\tau) \approx h^2 \sum_p A_p^2 \delta(\tau - \tau_p) . \quad (34)$$

The lowest peak is located at  $\tau = \tau_{min}$ , and for  $\tau \leq \tau_{min}$  the form factor is identically zero.

Based in Eqs.(29)–(34) we now make a simple qualitative analysis of the variance of the fluctuations of the thermodynamic functions. To simplify the analysis, in the chaotic case we will use the simple approximation (32) extended to times  $\tau \rightarrow \infty$ , and ignore the saturation of the form factor for longer times described by Eqs. (31). By doing this, we are overestimating the weight of the long orbits. To begin with, we also set the temperature to zero. In Table I we put  $\kappa_T = 1$  and  $\kappa'_T = 0$ . The variance of the entropy fluctuations therefore vanishes, as it should. We now discuss the non-vanishing quantities.

Consider for example the variance of the energy (or of the grand potential). From Eqs. (32) and (33) we see that for chaotic systems the integrand in Eq. (29) behaves as  $\tau^{-3}$ , while from Eqs. (30) and (33) it follows that for integrable motion the integrand varies as  $\tau^{-4}$ . Therefore in both cases the integral (29) converges for long times, even at zero temperature. The dominant contributions come in fact from short times, where the divergence of the integral is stopped by the cutoff at  $\tau = \tau_{min}$  introduced by the form factor. When applied to other thermodynamic quantities, the same analysis shows that the fluctuations of the response function for integrable and chaotic dynamics, and those of the particle number for integrable systems, are also dominated by the short-time contributions. Because the short-time dynamics is specific to each system, then in general the second moments of those functions are non-universal, and consequently the same is true for the probability distribution. This conclusion remains valid as the temperature increases, since a finite temperature truncates the long orbits.

We thus conclude that *the fluctuations of the grand potential, the energy and the response function for integrable and chaotic dynamics, and those of the particle number for integrable systems, are dominated, at an arbitrary temperature, by the shortest non-universal periodic orbits of the system.*

As mentioned before, the sum for  $\langle \tilde{N}^2 \rangle$  is convergent only for integrable systems. The analysis shows that the shortest orbits are not providing the dominant contribution when considering the fluctuations of the particle number of chaotic systems. The same conclusion is reached at low temperatures for other thermodynamic functions, like the entropy or the specific heat. As  $T \rightarrow 0$  the moments of the distribution of the fluctuations of these quantities pick up contributions from orbits with period  $\tau_p \gtrsim \tau_H$ , whose statistical behavior is universal. Conversely, in the energy domain the thermodynamic fluctuations of these quantities therefore depend on the statistical properties of the single-particle dynamics on a scale  $\leq \delta$ . To see this explicitly in a particular case, consider the second moment of the entropy, given from Eq.(29) and Table I by

$$\langle \tilde{S}^2 \rangle = \frac{\hbar^2}{2\pi^2} \int_0^\infty \frac{d\tau}{\tau^4} K(\tau) \kappa'_T{}^2(\tau) . \quad (35)$$

The function  $\kappa'_T(\tau)$  has a peak centered at  $\tau \approx \tau_T$  of height proportional to  $1/T$  (for  $\tau/\tau_T \rightarrow 0$  it vanishes as  $\kappa'_T(\tau) \approx -(\tau/\tau_T)^2/3T$ ). In the limit  $T \rightarrow 0$  this function therefore selects in the integral (35) arbitrarily long orbits. The variance of the entropy is therefore dominated by the long universal orbits whenever  $\tau_T \gg \tau_{min}$  or, equivalently, for temperatures  $k_B T \ll E_c/2\pi^2$ . On the contrary, for temperatures  $k_B T \approx E_c/2\pi^2$  non-universal orbits in the form factor are selected and the result will depend on the system-specific peculiarities of the short orbits. The explicit dependence of  $\langle \tilde{S}^2 \rangle$  on temperature will be computed below. Similar arguments may be applied to other quantities, like the specific heat. We therefore conclude that those functions have, at  $k_B T \ll E_c/2\pi^2$ , universal fluctuation distributions whose functional form depend only on the universality class of the local single-particle fluctuations on a scale  $\lesssim \delta$ .

#### IV. THE SECOND MOMENT IN THE $\tau_{MIN}$ -APPROXIMATION

There is in fact a simple way to estimate the variance in all the cases considered above, independently of the short or long-time origin of the dominant contributions. The approximation consists in using in Eq. (29) the appropriate statistical form factor (given by Eqs. (30) and (31) for integrable and chaotic motion, respectively), the corresponding

value of  $Q^2(\tau)$  from Eq. (33), and to put  $K(\tau) = 0$  for  $\tau < \tau_{min}$  in all cases. This is clearly an approximation, that we call the  $\tau_{min}$ -approximation, since we are extrapolating the statistical behavior of the orbits down to times  $\tau \approx \tau_{min}$ , ignoring the short-time system-dependent structures. All the short-time structures are condensed into a single parameter, the period of the shortest orbit. For the fluctuations of the thermodynamic quantities dominated by the shortest orbits – whose second moment is described more accurately below, see Eq. (44) – this is clearly a rough approximation. On the contrary, for the entropy at low temperatures, and for the variance of the particle number in chaotic systems, the leading order will be well described by this approximation while the error, as we shall now see, is made in the correction terms.

The virtue of the  $\tau_{min}$ -approximation is to provide simple estimates of the size of the fluctuations, as well as of their dependence with chemical potential, particle number, or external parameter. It requires a minimum amount of information of the system, and is thus of interest in the analysis of experiments.

### A. Zero temperature.

Setting  $\kappa_T = 1$  and  $\kappa'_T = 0$  in Eq.(29), in this approximation the results are expressed in terms of  $\tau_{min}$ , the parameters  $\alpha$  and  $\omega$  entering in Eq.(33), the shell strength  $g$  defined in Section II C, and the symmetry parameter  $\beta$  in chaotic systems. Since the integrals obtained from Eq.(29) are straightforward, we do not give here a detailed account of their computation. The results obtained are summarized in Table II. For chaotic systems with time reversal symmetry ( $\beta = 1$ ), only the leading order terms in  $1/g$  are included. The first row of the table also describes the variance of the grand potential.

	Integrable	Chaotic $\beta = 1$	Chaotic $\beta = 2$
$\langle \tilde{U}^2 \rangle$	$\frac{1}{24\pi^4} g E_c^2$	$\frac{1}{8\pi^4} E_c^2 \left( 1 - \frac{2}{g} + \mathcal{O}(g^{-2} \log g) \right)$	$\frac{1}{16\pi^4} E_c^2 \left( 1 - \frac{1}{3g^2} \right)$
$\langle \tilde{N}^2 \rangle$	$\frac{1}{2\pi^2} g$	$\frac{1}{\pi^2} \left( \log g + 1 - \frac{\pi^2}{8} + \mathcal{O}(g^{-1}) \right)$	$\frac{1}{2\pi^2} (\log g + 1)$
$\langle \tilde{R}^2 \rangle$	$\frac{1}{2\pi^2} \omega g$	$\frac{1}{\pi^2} \frac{\alpha}{\tau_{min}} \left( 1 - \frac{\log g}{g} + \mathcal{O}(g^{-1}) \right)$	$\frac{1}{2\pi^2} \frac{\alpha}{\tau_{min}} \left( 1 - \frac{1}{2g} \right)$

**Table II:** Zero-temperature second moments obtained in the  $\tau_{min}$ -approximation

From these results it is possible to establish the scaling of the variances with the Fermi energy and with the system size  $L$  for a gas contained in a  $d$ -dimensional cavity. We assume here that the parameter  $x$  entering in the definition of the response is a geometrical parameter that controls the shape of the cavity (other parameters can be treated likewise). Since  $\tau_{min} \propto L E_F^{-1/2}$ , then  $E_c \propto L^{-1} E_F^{1/2}$ . From Eqs. (12) and (13) (generalized to  $d$ -dimensions) we have  $\delta^{-1} \propto L^d E_F^{d/2-1}$ . It then follows that  $g \propto (L E_F^{1/2})^{d-1}$ . It has moreover been shown [20,21] that for shape deformations of a cavity  $\alpha \propto L^{-1} E_F^{3/2}$ , and  $\omega \propto L^{-2} E_F^2$ . Using these relations, we obtain the results summarized in Table III. The dependence with the number of fermions  $N$  in the gas has been computed assuming a constant density  $n = N/V$  of the gas. Therefore  $E_F$  remains constant and, according to Eq. (12), the size of the system increases like  $L \propto N^{1/d}$  with the number of particles. Different dependencies are obtained when the volume is kept fixed. It is also interesting to compare the typical quantum fluctuations to the magnitude of the average part. For instance, since at constant density  $\bar{U} \propto N$  (for any dimension) (cf [10]), then  $\sqrt{\langle \tilde{U}^2 \rangle} / \bar{U} \propto 1/N^{(d+3)/2d}$ .

	Integrable	Chaotic
$\langle \tilde{U}^2 \rangle$	$L^{d-3} E_F^{(d+1)/2} \sim N^{(d-3)/d}$	$L^{-2} E_F \sim N^{-2/d}$
$\langle \tilde{N}^2 \rangle$	$(L E_F^{1/2})^{d-1} \sim N^{(d-1)/d}$	$\log(L E_F^{1/2}) \sim \log N$
$\langle \tilde{R}^2 \rangle$	$L^{d-3} E_F^{(d+3)/2} \sim N^{(d-3)/d}$	$L^{-2} E_F^2 \sim N^{-2/d}$

**Table III:** Zero-temperature scaling of the variances with the system size  $L$ , Fermi energy, and with the number of particles  $N$  in the gas in a  $d$ -dimensional cavity (keeping the density fixed).

### B. Temperature dependence of the fluctuations

The variances depend on temperature through the function  $\kappa_T$  (or its derivative), contained in the function  $F(\tau)$  in Eq.(29). It would be too cumbersome to go through each function in detail. To be specific, we illustrate the results by computing the temperature dependence of the second moment of the entropy fluctuations, Eq.(35). In the  $\tau_{min}$ -approximation, Eq.(35) is written

$$\langle \tilde{S}^2 \rangle = \frac{k_B^2}{2} \int_0^\infty \frac{dx}{x^4} \left( \frac{x}{\sinh x} - \frac{x^2 \cosh x}{\sinh^2 x} \right)^2 K(x, x_H), \quad (36)$$

where  $K(x, x_H) = (1/\tau_T)K(\tau = x\tau_T)$ ,  $x_H = \tau_H/\tau_T$ , and  $K(x, x_H) = 0$  for  $x < x_{min}$ , where  $x_{min} = \tau_{min}/\tau_T$ .

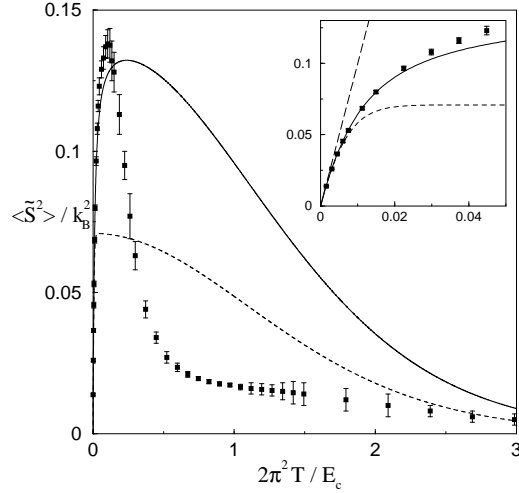


FIG. 1. Temperature dependence of the entropy fluctuations in chaotic systems, with  $g = 130$ . Full and dashed lines: Eq. (36) ( $\tau_{min}$ -approximation) for  $\beta = 1$  and  $\beta = 2$ , respectively. Squares: Fermi gas in a Sinai cavity. The inset shows the behavior close to the origin. The long-dashed straight line corresponds to Eq.(39).

In *chaotic* systems three different temperature regimes can be distinguished.

\* *Low temperatures:*  $k_B T \ll \delta/2\pi^2$ . In this regime the function  $\kappa'_T(\tau)$  is centered at times much larger than  $\tau_H$ . We therefore ignore all the structure of the form factor at finite  $\tau$  and take the asymptotic limit  $K(x, x_H) \approx x_H$  in Eq.(36). Then

$$\langle \tilde{S}^2 \rangle = \frac{k_B^2 x_H}{2} \int_0^\infty \frac{dx}{x^4} \left( \frac{x}{\sinh x} - \frac{x^2 \cosh x}{\sinh^2 x} \right)^2. \quad (37)$$

Denoting

$$I_k = \int_0^\infty \frac{dx}{x^k} \left( \frac{x}{\sinh x} - \frac{x^2 \cosh x}{\sinh^2 x} \right)^2, \quad (38)$$

the variance of the entropy in the low temperature regime grows like

$$\langle \tilde{S}^2 \rangle = \frac{1}{2} I_4 k_B^2 \frac{k_B T}{(\delta/2\pi^2)}, \quad (39)$$

where  $I_4 \approx 0.153842$ . The variance therefore increases linearly with temperature, with a slope proportional to the average single-particle density of states. It is interesting to remark that, up to a constant prefactor, the low-temperature

growth of the quantum fluctuations agrees with that of the thermal fluctuations of the gas, which are of completely different physical origin [10]. It is also interesting to compare the typical size of the quantum fluctuations to their average part. From Eq.(39) we have  $\sqrt{\langle \tilde{S}^2 \rangle} = \sqrt{I_4/2} k_B \sqrt{k_B T / (\delta/2\pi^2)}$ , to be compared to the (low-temperature) growth of the average part  $\bar{S} = (1/6)k_B(k_B T / (\delta/2\pi^2))$ .

\* *Intermediate temperatures:*  $\delta/2\pi^2 \ll k_B T \ll E_c/2\pi^2$ . In this regime the form factor may be approximated by its linear behavior, Eq.(32). Using moreover the  $\tau_{min}$  approximation for the integral we get from Eq. (36)

$$\langle \tilde{S}^2 \rangle = \frac{1}{\beta} I_3 k_B^2 - \frac{1}{18\beta} k_B^2 \left( \frac{k_B T}{E_c/2\pi^2} \right)^2, \quad (40)$$

where  $I_3 = 0.141832$ . There is therefore a saturation of the magnitude of the entropy fluctuations in this intermediate regime at the “quantum of entropy”  $\sqrt{\langle \tilde{S}^2 \rangle} \approx k_B$ , with a weak negative quadratic dependence on temperature. Notice also the inverse dependence on the symmetry parameter  $\beta$ , which is absent in Eq. (39).

\* *High temperatures:*  $k_B T \gg E_c/2\pi^2$ . Since the form factor is different from zero for times  $\tau \geq \tau_{min}$ , in this limit we can approximate the function  $\kappa'_T(\tau)$  by its exponential tail  $\kappa'_T(\tau) \approx -(2/T)(\tau/\tau_T)^2 \exp(-\tau/\tau_T)$ . Then, in the  $\tau_{min}$ -approximation and using again the linear short-time behavior of  $K(\tau)$  we find

$$\langle \tilde{S}^2 \rangle = \frac{1}{\beta} k_B^2 \left[ 1 + 2 \left( \frac{k_B T}{E_c/2\pi^2} \right) \right] e^{-2k_B T / (E_c/2\pi^2)}. \quad (41)$$

At high temperatures compared to  $E_c$  we thus observe the expected exponential decay of the quantum fluctuations due to the thermal smoothing.

The behavior of the entropy fluctuations as a function of temperature computed from Eq. (36) for chaotic systems in this approximation is displayed in Fig. 1 for the two symmetry classes.

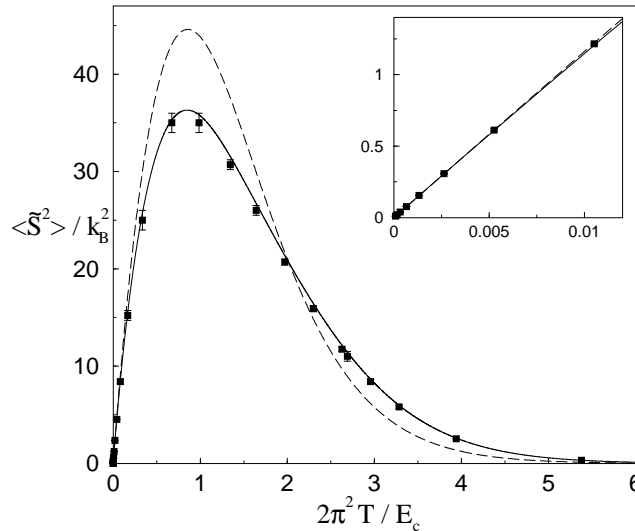


FIG. 2. Temperature dependence of the entropy fluctuations in regular systems, with  $g = 1500$ . Long-dashed line: Eq. (36) ( $\tau_{min}$ -approximation). Squares: Fermi gas in a rectangular cavity. Full line: semiclassical sum over periodic orbits, Eq.(44). The inset shows the behavior close to the origin.

The situation is different in *integrable systems* due to the different behavior of the form factor, Eq.(30). Accordingly, there are only two temperature regimes.

\* *Low temperatures:*  $k_B T \ll E_c/2\pi^2$ . In this regime the form factor is approximated by its asymptotic value  $\tau_H$ , ignoring its short-time structure. The result is identical to the low temperature regime of chaotic systems, Eq.(39). The main difference with respect to the chaotic case is that now this linear growth extends up to temperatures of order  $E_c/2\pi^2$  instead of  $\delta/2\pi^2$ . At this temperature, the typical entropy fluctuations  $\sqrt{\langle \tilde{S}^2 \rangle}$  are of order  $\sqrt{gk_B^2}$ , which

are a factor  $\sqrt{g} \gg 1$  greater than the maximum fluctuations in chaotic systems.

\* *High temperatures:*  $k_B T \gg E_c/2\pi^2$ . As in chaotic systems, the function  $\kappa'_T(\tau)$  is approximated by its exponential tail, and use is made of the  $\tau_{min}$  approximation for the form factor,  $K(\tau) = 0$  for  $\tau < \tau_{min}$  and  $K(\tau) = \tau_H$  for  $\tau > \tau_{min}$ . We get

$$\langle \tilde{S}^2 \rangle = k_B^2 \left( \frac{k_B T}{\delta/2\pi^2} \right) e^{-2k_B T/(E_c/2\pi^2)}. \quad (42)$$

Fig. 2 shows, in this approximation, the behavior of the second moment of the entropy fluctuations in integrable systems.

The second moment of the entropy fluctuations computed in the  $\tau_{min}$ -approximation are expected to be accurate in the regime  $2\pi^2 k_B T \lesssim \delta$ , where only long orbits (compared to  $\tau_{min}$ ) contribute. This is confirmed by comparing with numerical simulations of a Fermi gas in a cavity. Two different geometries are considered (cf Fig. 3). In the first, a Fermi gas is contained inside a 2D cavity with infinite wall potential having a Sinai shape. The corresponding classical single-particle motion is fully chaotic. The second is similar, but the cavity has a rectangular shape. This guarantees an integrable single-particle dynamics. The results obtained for the numerical simulations of a Fermi gas in these two geometries are plotted in Figs. 1 and 2 (squares). A good agreement is observed indeed in the regime  $2\pi^2 k_B T \lesssim \delta$  (cf the insets).

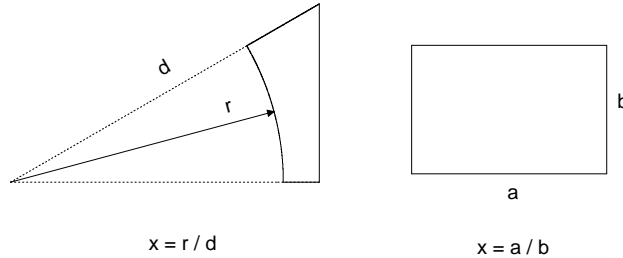


FIG. 3. Cavities used to confined the Fermi gas. Left: Sinai (chaotic). Right: rectangle (integrable). The parameter  $x$  as defined in each case is varied to modify the shape (while keeping the area constant).

As temperature increases, shorter orbits become relevant for the entropy fluctuations. For temperatures  $2\pi^2 k_B T \approx E_c$  or higher the  $\tau_{min}$ -approximation fails because a statistical treatment of the orbits is not appropriate any more. These deviations are clearly seen in Figs. 1 and 2. In this range a precise description of the decay of the fluctuations requires to explicitly take into account the different short periodic orbits of the single-particle motion, which are dominant. This treatment, which requires a much more detailed knowledge about the system than the simple  $\tau_{min}$ -approximation, is considered in the following section (V B). It produces in the case of the rectangular cavity the much more accurate description represented by the full curve in Fig. 2.

The temperature dependence of other thermodynamic quantities may be computed analogously. For example, the second moment of the energy of chaotic systems shows a quadratic decrease up to temperatures  $k_B T \approx E_c/2\pi^2$ , followed by an exponential tail for temperatures  $k_B T \gg E_c/2\pi^2$ . A qualitatively similar behavior is obtained for integrable systems. The temperature dependence of the second moment of the particle number and of the response function may be computed similarly.

## V. HIGHER MOMENTS AND DISTRIBUTIONS

### A. Universal thermodynamic fluctuations

In this case the fluctuations can be directly related to the local universal statistics of the single-particle energy levels. The latter correspond to an uncorrelated sequence for integrable systems, and to a random matrix sequence in the chaotic case. This type of fluctuations are observed in some thermodynamic functions at temperatures  $k_B T \ll E_c/(2\pi^2)$ .

The simplest quantity having a universal distribution at low temperatures is the particle number in chaotic systems with a fixed chemical potential. It has been conjectured that at zero temperature the fluctuations of the particle number in chaotic systems are Gaussian distributed [23] (cf part (b) of Fig 7). Since the variance of  $\tilde{N}$  was already computed in Section IV, the distribution is completely fixed in the range  $k_B T \ll E_c/2\pi^2$  where the universality holds.

Another thermodynamic function having universal fluctuations that we consider here in detail is the entropy. When expressed in terms of the single-particle energy levels  $E_j$ , this function, defined by Eq.(8), takes the form

$$S(x, \mu, T) = k_B \sum_j \log \left[ 1 + e^{(\mu - E_j)/k_B T} \right] - \frac{1}{T} \sum_j \frac{\mu - E_j}{1 + e^{(E_j - \mu)/k_B T}}. \quad (43)$$

At zero temperature, and as a function of the chemical potential,  $S(x, \mu, T)$  vanishes everywhere except when  $\mu = E_j$ ,  $j = 1, 2, \dots$ , where it takes the value  $S = k_B \log 2$ . As temperature increases, peaks of width proportional to  $T$  centered at  $\mu = E_j$  develop. At a given chemical potential  $\mu$ , the entropy is therefore the superposition of the contribution of the different peaks. In the range  $k_B T \ll \delta/2\pi^2$  this superposition is only determined by the neighboring energy levels  $E_j \approx \mu$ , and by their local statistical properties. We thus see, in a direct manner, that at low temperatures the statistical properties of the entropy depend only on the local statistics of the single-particle energy levels. The second moment of that distribution as a function of temperature was computed in Section IV.

To compute the full distribution for regular and chaotic dynamics in the range  $k_B T \ll E_c/2\pi^2$  one therefore has to compute the distribution of the entropy  $S$  from Eq.(43) by assuming an uncorrelated distribution and a random matrix distribution for the  $E_j$ 's, respectively. We have done a numerical computation of those probability distributions as a function of temperature. The results obtained are summarized in Figs. 4 and 5.

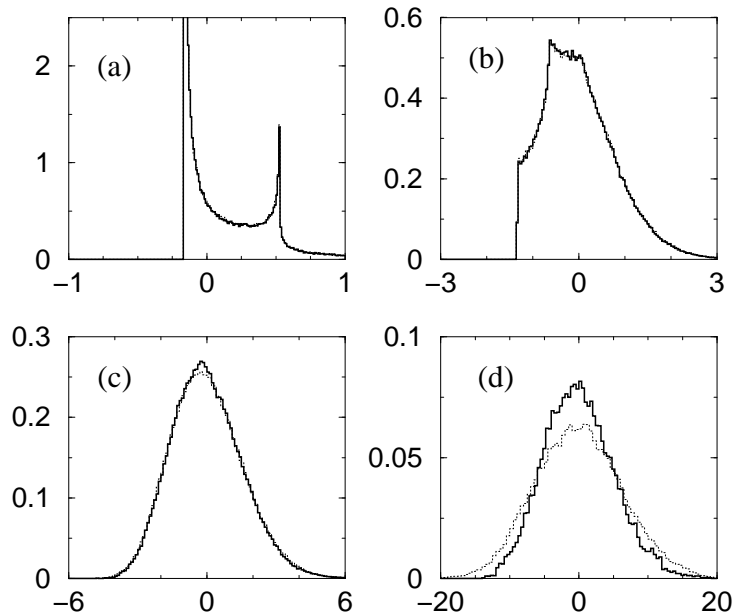


FIG. 4. Histogram of the entropy probability distribution for integrable single-particle motion at different temperatures. Dotted line: uncorrelated spectrum. Full line: Fermi gas in a rectangular box with  $x = (\sqrt{5} + 1)/2$ ,  $\mu = (5.75 \pm 0.75) \times 10^6$ , and  $g \approx 1500$ . (a)  $k_B T = \delta/(2\pi^2)$ ; (b)  $k_B T = 8 \times \delta/(2\pi^2)$ ; (c)  $k_B T = 32 \times \delta/(2\pi^2)$ ; (d)  $k_B T = 512 \times \delta/(2\pi^2) \approx (1/3)E_c/(2\pi^2)$ . In parts (a), (b) and (c) the two curves are almost indistinguishable.

Figure 4 compares the distribution of the entropy fluctuations obtained from Eq. (43) when the single-particle energy levels  $E_j$  are assumed to be uncorrelated with the probability distributions computed for a Fermi gas in a rectangular box. For temperatures up to  $2\pi^2 k_B T \approx 30\delta \approx E_c/50$  (part (a), (b), and (c)), the two distributions are almost indistinguishable and show a high sensitivity to temperature variations. For temperatures of the order  $E_c/2\pi^2$  or higher (part (d) of Fig. 4) the universality of the probability distribution is lost and strong deviations are observed. The entropy probability distribution for the uncorrelated spectrum tends to a Gaussian.

Figure 5 shows a similar comparison but for a chaotic single-particle dynamics. It compares the probability distribution of the entropy fluctuations computed from Eq. (43) when the single-particle energy levels  $E_j$  are eigenvalues of a random matrix ensemble with  $\beta = 1$ , with the probability distribution computed for a Fermi gas in a Sinai box. Again, a remarkable agreement is found for temperatures  $2\pi^2 k_B T \ll E_c$ , and departures are observed as  $E_c$  is approached. The entropy probability distribution for the random matrix spectrum tends to a Gaussian.

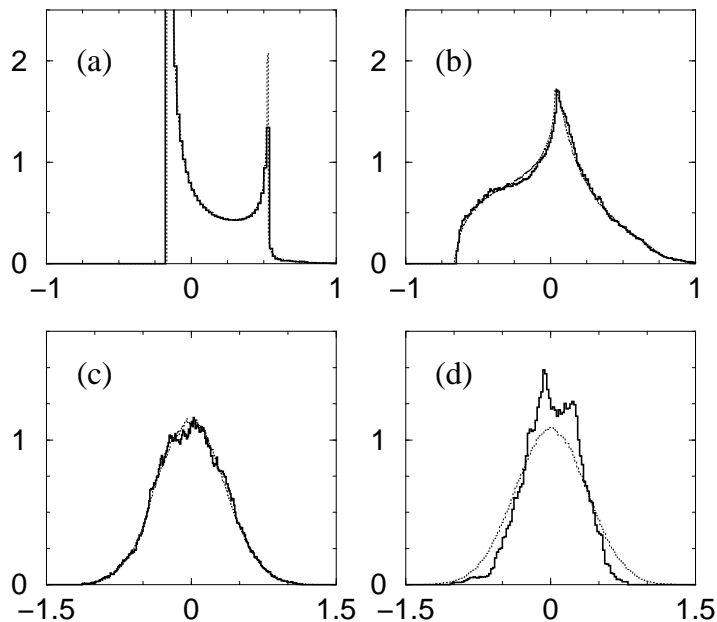


FIG. 5. Histogram of the entropy probability distribution for chaotic single-particle motion at different temperatures. Dotted line: random matrix spectrum ( $\beta = 1$ ). Full line: Fermi gas in a Sinai box with  $r = 0.765 \pm 0.0025$ ,  $\mu = 900 \pm 100$ , and  $g \approx 130$ . (a)  $k_B T = \delta/(2\pi^2)$ ; (b)  $k_B T = 4 \times \delta/(2\pi^2)$ ; (c)  $k_B T = 8 \times \delta/(2\pi^2)$ ; (d)  $k_B T = 32 \times \delta/(2\pi^2) \approx (1/4)E_c/(2\pi^2)$ .

For temperatures of order  $E_c/2\pi^2$  or higher (part (d) in Figs. 4 and 5), where the universality is lost, the moments of the probability distributions, which are now determined by the short periodic orbits, are non-universal and may be computed using the techniques developed below. One should keep in mind that the scale  $E_c$  and the shell-strength parameter  $g$ , set in a real system by the inverse time of flight across the system, are totally absent and therefore not defined in a purely uncorrelated or random matrix spectrum.

### B. Non-universal thermodynamic fluctuations

They occur when the fluctuations are dominated by the non-universal aspects of the short time dynamics. This type of fluctuations are observed in all the thermodynamic quantities for temperatures  $k_B T \geq E_c/(2\pi^2)$ . But they also occur, as we saw in section III, in certain thermodynamic functions at arbitrary temperatures (including  $T = 0$ ). The  $\tau_{min}$ -approximation used in Section IV to compute the second moment is not very accurate in this case since that approximation is too crude. Here we provide accurate expressions to compute all the moments of the distribution for non-universal fluctuations.

Since off diagonal terms involving different short periodic orbits in products like Eq. (27) are killed by the average procedure, the dominant contribution to the double sum will come from the rapidly convergent diagonal terms  $p = p'$ . From Eq. (27) the dominant diagonal contribution to the second moment of thermodynamic quantities with non-universal fluctuations, that we denote by a subscript “0”, is

$$\langle \tilde{\Phi}_0^2 \rangle = 2 \mathcal{C}^2 \sum_{p,r} \mathcal{A}_{p,r}^2 . \quad (44)$$

The advantage of the  $\tau_{min}$ -approximation computed in the previous section compared to the more accurate expression Eq.(44) is that only information about the period of the shortest orbit is required, while Eq.(44) involves much more detailed information about the periodic orbits.

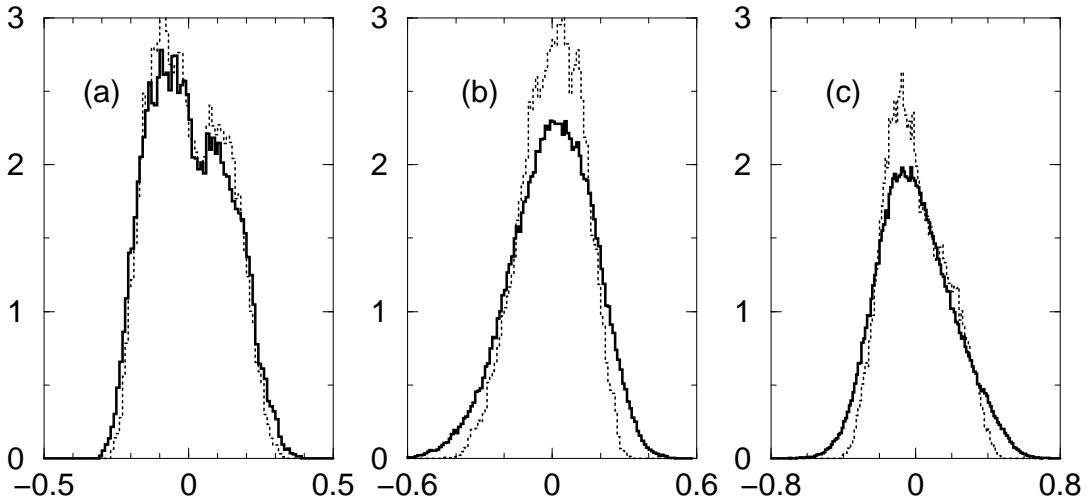


FIG. 6. Histogram of the probability distribution of normalized thermodynamic functions for a Fermi gas in a 2D rectangular box: (a)  $\tilde{U}/\mu^{3/4}$ , (b)  $\tilde{N}/\mu^{1/4}$ , (c)  $\tilde{R}/\mu^{5/4}$ . The distributions are computed at  $x = (1 + \sqrt{5})/2$ , in the window  $\mu = (1 \pm 0.1) \times 10^8$  ( $g = 1500$ ). Full line:  $T = 0$ . Dashed line:  $k_B T = 1273 \times \delta / (2\pi^2) \sim 0.5 \times E_c / (2\pi^2)$ .

The diagonal approximation Eq. (44) can be generalized to compute all the moments of the oscillating quantities. Unlike the variance, a main difference concerning the higher moments is that the repetitions of the periodic orbits play now an essential role. We will explicitly go through the calculation of the third and fourth moments, the generalization to the higher ones being straightforward. We return to the notation of equation (20), keeping in mind the dependence on chemical potential, parameter and temperature of the variables, but not writing it explicitly. By the semiclassical formula the third power is written as a triple sum

$$\tilde{\Phi}^3 = \mathcal{C}^3 \sum_{p_1, r_1} \mathcal{A}_{p_1, r_1} 2 \cos \alpha_{p_1, r_1} \sum_{p_2, r_2} \mathcal{A}_{p_2, r_2} 2 \cos \alpha_{p_2, r_2} \sum_{p_3, r_3} \mathcal{A}_{p_3, r_3} 2 \cos \alpha_{p_3, r_3} , \quad (45)$$

where  $\alpha_{p_i, r_i} = r_i S_{p_i} / \hbar + \nu_{p_i, r_i}$ . The product of three cosines gives

$$8 \cos \alpha_{p_1, r_1} \cos \alpha_{p_2, r_2} \cos \alpha_{p_3, r_3} = 2 \cos(\alpha_{p_1, r_1} + \alpha_{p_2, r_2} + \alpha_{p_3, r_3}) + 2 \cos(\alpha_{p_1, r_1} + \alpha_{p_2, r_2} - \alpha_{p_3, r_3}) \\ + 2 \cos(\alpha_{p_1, r_1} - \alpha_{p_2, r_2} + \alpha_{p_3, r_3}) + 2 \cos(\alpha_{p_1, r_1} - \alpha_{p_2, r_2} - \alpha_{p_3, r_3}) .$$

The average kills the first term in the r.h.s.. The last three terms give the same result interchanging indices. Then

$$\langle \tilde{\Phi}^3 \rangle = 6 \mathcal{C}^3 \left\langle \sum_{p_1, r_1} \sum_{p_2, r_2} \sum_{p_3, r_3} \mathcal{A}_{p_1, r_1} \mathcal{A}_{p_2, r_2} \mathcal{A}_{p_3, r_3} \cos(\alpha_{p_1, r_1} + \alpha_{p_2, r_2} - \alpha_{p_3, r_3}) \right\rangle_{\mu, x} . \quad (46)$$

The main dependence of this function on the chemical potential comes, as usual, from the variations of the argument  $\Delta\phi$  of the cosine. In the averaging window it is enough to consider a linear approximation

$$\Delta\phi = (r_1 \tau_{p_1} + r_2 \tau_{p_2} - r_3 \tau_{p_3}) \frac{\Delta\mu}{\hbar} . \quad (47)$$

The wild oscillatory behavior produced by the phase variations will typically have zero average, except for those terms for which  $\Delta\phi = 0$ . Assuming incommensurability of the periods of all the orbits, the only way to satisfy this condition is by imposing

$$\tau_{p_1} = \tau_{p_2} = \tau_{p_3} , \quad r_1 + r_2 = r_3 . \quad (48)$$

This is a generalization of the diagonal approximation, and illustrates the basic mechanism to calculate the higher moments. In the argument of the cosine in Eq. (46) only the Maslov indices survive because the equality of the periods implies the equality of the actions. The above constraints simplify the multiple sums and finally a compact expression for the third moment is obtained

$$\langle \tilde{\Phi}_0^3 \rangle = 6 \mathcal{C}^3 \sum_p \sum_{r_1=1}^{\infty} \sum_{r_2=1}^{\infty} \mathcal{A}_{p, r_1} \mathcal{A}_{p, r_2} \mathcal{A}_{p, r_1+r_2} \cos(\nu_{p, r_1} + \nu_{p, r_2} - \nu_{p, r_1+r_2}) . \quad (49)$$



When the fluctuations are dominated by the short orbits, the convergence of this series is guaranteed by the same arguments that showed the convergence of the second moment. The sum (49) is in general different from zero. This produces a finite skew giving a non-symmetric probability distribution.

$k$	$\tilde{U}/\mu^{3/4}$		$\tilde{N}/\mu^{1/4}$		$\tilde{R}/\mu^{5/4}$	
	$T = 0$	$T_1 \neq 0$	$T = 0$	$T_1 \neq 0$	$T = 0$	$T_1 \neq 0$
2	$(1.81 \pm 0.01) \times 10^{-2}$ $1.83290 \times 10^{-2}$	$(1.55 \pm 0.01) \times 10^{-2}$ $1.57853 \times 10^{-2}$	$(2.83 \pm 0.05) \times 10^{-2}$ $2.8477 \times 10^{-2}$	$(1.63 \pm 0.03) \times 10^{-2}$ $1.65251 \times 10^{-2}$	$(4.25 \pm 0.10) \times 10^{-2}$ $4.3148 \times 10^{-2}$	$(2.84 \pm 0.06) \times 10^{-2}$ $2.89043 \times 10^{-2}$
3	$(5.0 \pm 0.4) \times 10^{-4}$ $5.31694 \times 10^{-4}$	$(3.5 \pm 0.5) \times 10^{-4}$ $3.81036 \times 10^{-4}$	$-(1.3 \pm 0.2) \times 10^{-3}$ $-1.35453 \times 10^{-3}$	$-(5.5 \pm 0.7) \times 10^{-4}$ $-5.85974 \times 10^{-4}$	$(2.4 \pm 0.3) \times 10^{-3}$ $2.44332 \times 10^{-3}$	$(1.6 \pm 0.1) \times 10^{-3}$ $1.58641 \times 10^{-3}$
4	$(7.1 \pm 0.2) \times 10^{-4}$ $7.3133 \times 10^{-4}$	$(4.95 \pm 0.05) \times 10^{-4}$ $5.13214 \times 10^{-4}$	$(2.3 \pm 0.1) \times 10^{-3}$ $2.33807 \times 10^{-3}$	$(6.8 \pm 0.3) \times 10^{-4}$ $7.14034 \times 10^{-4}$	$(5.0 \pm 0.3) \times 10^{-3}$ $5.16324 \times 10^{-3}$	$(1.9 \pm 1.0) \times 10^{-3}$ $1.99110 \times 10^{-3}$

**Table IV:** Moments of the distribution of some thermodynamic functions with non-universal fluctuations for a Fermi gas in a rectangular cavity. In each row, the upper values are the numerical results obtained from the distributions shown in Fig. 6, while the lower values are obtained from the semiclassical sums over periodic orbits. The temperature  $T_1 = k_B T = 1273 \times \delta / (2\pi^2)$  is the same as in Fig. 6.

The fourth moment is calculated in a similar way. The product of four cosines gives eight terms. One of them, containing the sum of all the actions, has zero average. The other terms, arranged after interchanging indices, give

$$\begin{aligned} \langle \tilde{\Phi}^4 \rangle = 2 \mathcal{C}^4 & \left\langle \sum_{p_1, r_1} \cdots \sum_{p_4, r_4} \mathcal{A}_{p_1, r_1} \mathcal{A}_{p_2, r_2} \mathcal{A}_{p_3, r_3} \mathcal{A}_{p_4, r_4} \left[ 4 \cos(\alpha_{p_1, r_1} + \alpha_{p_2, r_2} + \alpha_{p_3, r_3} - \alpha_{p_4, r_4}) \right. \right. \\ & \left. \left. + 3 \cos(\alpha_{p_1, r_1} + \alpha_{p_2, r_2} - \alpha_{p_3, r_3} - \alpha_{p_4, r_4}) \right] \right\rangle. \end{aligned} \quad (50)$$

We restrict again to those terms having exactly zero phase variation, neglecting quasi cancellations of long orbits. Then for the first cosine in the r.h.s. this is equivalent to  $r_1 \tau_{p_1} + r_2 \tau_{p_2} + r_3 \tau_{p_3} - r_4 \tau_{p_4} = 0$ , and by the incommensurability of the periods the only solution is

$$p_1 = p_2 = p_3 = p_4, \quad r_1 + r_2 + r_3 = r_4. \quad (51)$$

As for the third cosine, this condition gives a simple sum over primitive periodic orbits. The three indices  $r_1, r_2$  and  $r_3$  are free, and  $r_4$  is determined by them.

For the second cosine the corresponding equation  $r_1 \tau_{p_1} + r_2 \tau_{p_2} - r_3 \tau_{p_3} - r_4 \tau_{p_4} = 0$  admits two different solutions. The first one is

$$p_1 = p_2 = p_3 = p_4, \quad r_1 + r_2 = r_3 + r_4. \quad (52)$$

The difference is that only  $r_1$  and  $r_2$  are free. Because the repetitions are positive integer numbers,  $r_3$  varies between 1 and  $r_1 + r_2 - 1$ , and  $r_4$  is determined by the constraint. The other solution, which has a weight two because of the possibility of interchanging indices, is

$$p_3 = p_1, \quad p_4 = p_2, \quad r_3 = r_1, \quad r_4 = r_2. \quad (53)$$

This reduces the expressions to double sums over two different primitive periodic orbits,  $p_1$  and  $p_2$ , and the repetitions  $r_1, r_2$ . To eliminate the inequality between  $p_1$  and  $p_2$ , we can add and subtract a term where the two indices are equal. With this term the double sum, both in primitive periodic orbits and repetitions, factorizes giving a term directly proportional to the square of the second moment, in its diagonal approximation. Finally we arrive at a convergent formula for the fourth moment

$$\begin{aligned} \langle \tilde{\Phi}_0^4 \rangle = 2 \mathcal{C}^4 & \sum_p \left[ 4 \sum_{r_1, r_2, r_3=1}^{\infty} \mathcal{A}_{p, r_1} \mathcal{A}_{p, r_2} \mathcal{A}_{p, r_3} \mathcal{A}_{p, r_1+r_2+r_3} \cos(\nu_{p, r_1} + \nu_{p, r_2} + \nu_{p, r_3} - \nu_{p, r_1+r_2+r_3}) \right. \\ & + 3 \sum_{r_1, r_2=1}^{\infty} \sum_{r_3=1}^{r_1+r_2-1} \mathcal{A}_{p, r_1} \mathcal{A}_{p, r_2} \mathcal{A}_{p, r_3} \mathcal{A}_{p, r_1+r_2-r_3} \cos(\nu_{p, r_1} + \nu_{p, r_2} - \nu_{p, r_3} - \nu_{p, r_1+r_2-r_3}) \\ & \left. - 6 \sum_{r_1, r_2=1}^{\infty} \mathcal{A}_{p, r_1}^2 \mathcal{A}_{p, r_2}^2 \right] + 3 \langle \tilde{\Phi}^2 \rangle^2. \end{aligned} \quad (54)$$

The last term  $3\langle\tilde{\Phi}^2\rangle^2$  is the result for the fourth moment if the distribution would have been Gaussian. The remaining terms in Eq. (54) produce deviations from that behavior (the excess of the distribution).

The generalization to higher moments is straightforward. The formulae are more complex, but they are always written as a sum over one primitive periodic orbit index, the repetitions originating from different constraints, plus terms coming from the previous moments (e.g. for the fifth moment there is a term proportional to  $\langle\tilde{\Phi}^2\rangle\langle\tilde{\Phi}^3\rangle$ ).

Figures 6 and 7 illustrate these results. They show the distribution of the quantum fluctuations of the total energy, particle number and response of a Fermi gas contained in a 2D rectangular and Sinai cavity, respectively. The fluctuating part of the thermodynamic functions is normalized by an appropriate power of the chemical potential. This normalization eliminates their zero-temperature energy dependence (cf Table III with  $d = 2$ ). The probability distributions are normalized by setting their area to one. The parameter  $x$  used to compute the response controls the shape of the cavity (cf Fig. 3), while the area is kept constant.  $R$  is therefore a “quantum” force, related to the variations of the energy of the gas produced by the quantum shell corrections.

The first four moments of the probability distributions shown in Fig. 6 have been computed. The numerical results obtained, at the two different temperatures, are compared in Table IV to the first four moments calculated using the analytic expressions obtained above based on the periodic orbits. The overall precision obtained is of the order of 2% (in the worst case), and is within the numerical uncertainties. For comparison, the rescaled second moments of the energy, particle number and response computed at  $T = 0$  using the  $\tau_{min}$ -approximation are  $1.74 \times 10^{-2}$ ,  $3.2 \times 10^{-2}$  and  $3.98 \times 10^{-2}$ , respectively. They have an accuracy of 4%, 13% and 6% with respect to the numerical values of Table IV, respectively.

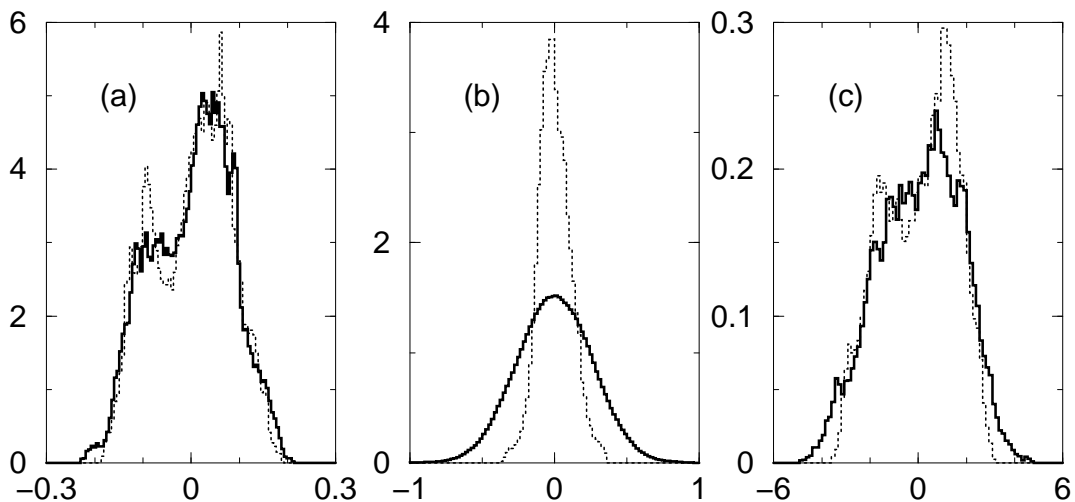


FIG. 7. Histogram of the probability distribution of normalized thermodynamic functions for a Fermi gas in a 2D Sinai box: (a)  $\tilde{U}/\mu^{3/4}$ , (b)  $\tilde{N}/\mu^{1/4}$ , (c)  $\tilde{R}/\mu^{5/4}$ . The distributions are computed in the windows  $r = 0.765 \pm 0.0006$ ,  $\mu = 750 \pm 250$ . Full line:  $T = 0$ . Dashed line:  $k_B T = 0.2 \times E_c / (2\pi^2)$ .

We have also computed from Eq. (44) the temperature dependence of the variance of the entropy fluctuations for a Fermi gas in the rectangular box using the shortest orbits. The result is represented by the full line in Fig. 2, which shows a very good agreement with respect to the numerical values computed directly from the Fermi gas. Such a good agreement is found even at temperatures of order  $\delta$  because, in integrable systems, the “diagonal” approximation used above is almost exact. This is not expected to occur in chaotic systems. We were not able to make similar comparisons for the chaotic Sinai cavity because we haven’t computed the periodic orbits for that system.

The fluctuations of the particle number in the chaotic case, Fig. 7(b), shows at  $T = 0$  the universal Gaussian behavior discussed in section V.A. At higher temperatures the universality is lost.

## VI. CORRELATION FUNCTIONS

When the parameter  $x$  or chemical potential  $\mu$  are varied, the autocorrelation function of a thermodynamic quantity  $\Phi$  is defined as

$$C_\Phi(x, \mu) = \left\langle \tilde{\Phi}(x_0 - x/2, \mu_0 - \mu/2, T) \tilde{\Phi}(x_0 + x/2, \mu_0 + \mu/2, T) \right\rangle_{x_0, \mu_0}. \quad (55)$$

In the following, we assume that the regular or chaotic nature of the single-particle motion in the gas is unchanged when the parameters  $(x_0, \mu_0)$  vary. When  $\Phi$  is expressed as a sum over the periodic orbits using Eq.(20),  $C_\Phi$  takes the form of a double sum over periodic orbits labelled by the indices  $p$  and  $p'$ . As usual, only the term involving one half the cosine of the difference of the actions gives a non-zero average. The amplitudes  $\mathcal{A}_p$  and actions  $S_p$  are evaluated at  $(\mu_0 - \mu/2, x_0 - x/2)$ , while those with index  $p'$  at  $(\mu_0 + \mu/2, x_0 + x/2)$ . In the semiclassical regime these functions will have a slow variation in a quantum scale, and therefore to leading order the parameter dependence can be ignored in the prefactors, and only a linear expansion of the actions is taken

$$S_p(\mu_0 \pm \frac{\mu}{2}, x_0 \pm \frac{x}{2}) \approx S_p(\mu_0, x_0) \pm \frac{\tau_p \mu}{2} \pm \frac{Q_p x}{2}.$$

The autocorrelation is now written

$$C_\Phi(x, \mu) = 2 \mathcal{C}^2 \left\langle \sum_{p,p'} \sum_{r,r'=1}^{\infty} \mathcal{A}_{p,r} \mathcal{A}_{p',r'} \cos \left[ \frac{rS_p - r'S_{p'}}{\hbar} + \frac{(r\tau_p + r'\tau_{p'})}{2\hbar} \mu + \frac{(rQ_p + r'Q_{p'})}{2\hbar} x \right] \right\rangle, \quad (56)$$

where all the classical functions are evaluated at  $(x_0, \mu_0)$ . The average over a small window  $\Delta x$  around  $x_0$  restricts the sums to orbits having approximately the same  $Q_p$ , while the energy average imposes the same condition over the periods.

To proceed further there are two main paths, corresponding to universal and non-universal fluctuations. For the latter, since short orbits dominate, the diagonal approximation furnishes the main contribution to the autocorrelation,

$$C_{\Phi,0}(x, \mu) = 2 \mathcal{C}^2 \sum_p \sum_{r=1}^{\infty} \mathcal{A}_{p,r}^2 \cos \left( \frac{r Q_p x}{\hbar} + \frac{r \tau_p \mu}{\hbar} \right). \quad (57)$$

In this equation the shortest periodic orbits have the largest prefactors  $\mathcal{A}_{p,r}$  and the lowest frequencies inside the cosine, giving rise in general to an erratic and non-decaying oscillation as a function of the parameters. The typical period of these oscillations is dominated by the shortest periodic orbit. The correlation lengths, both in chemical potential and external parameter  $x$  are estimated making the phase variation equal to  $2\pi$  giving

$$\mu^* = E_c = \frac{\hbar}{\tau_{min}} \quad x^* = \frac{\hbar}{|Q_{min}|}. \quad (58)$$

In the presence of universal fluctuations, the treatment of Eq.(56) is different. Since long orbits give an important contribution, the diagonal approximation is not sufficient and a more accurate evaluation is needed. General expressions for the autocorrelation of the gas were given in Ref. [21]. Ordering the orbits by their period, and taking into account the restrictions imposed by the averaging procedure, the autocorrelation of a thermodynamic quantity  $\Phi$  takes the form

$$C_\Phi(x, \mu) = \frac{\mathcal{C}^2}{2\pi^2 \hbar^2} \int_0^\infty \frac{d\tau}{\tau^4} \cos(\mu\tau/\hbar) K(\tau, x) F(\tau). \quad (59)$$

The constant  $\mathcal{C}$  and the function  $F(\tau)$  are defined as in Eq.(29), to which Eq.(59) reduces when  $x = \mu = 0$  ( $K(\tau, x = 0) = K(\tau)$ ). The function  $K(\tau, x)$  is a generalization of the form factor: it is the Fourier transform of the parametric two-point correlation function  $\langle \tilde{\rho}(\mu_0 - \mu/2, x_0 - x/2) \tilde{\rho}(\mu_0 + \mu/2, x_0 + x/2) \rangle_{\mu_0}$  with respect to  $\mu$ . Semiclassically its expression is given by Eq.(28) with the replacement  $\cos[(S_p - S_{p'})/\hbar] \rightarrow \cos[(S_p - S_{p'})/\hbar + (Q_p + Q_{p'})/2\hbar]$ . For chaotic systems and for times  $\tau \gg \tau_{min}$ ,  $K(\tau, x)$  has been conjectured to be a universal function depending only on the symmetry parameter  $\beta$  and described by random matrix theory [24].

In many cases this integral may lead to results which are determined only by the universal, long time aspects of the dynamics. Consider for example the autocorrelation of the entropy. Then  $F(\tau) = \kappa_T'^2(\tau)$  in Eq.(59). At temperatures  $k_B T \ll E_c/2\pi^2$  the function  $\kappa_T'^2(\tau)$  selects only times much longer than  $\tau_{min}$ . Then the integral in (59) is insensitive to the system-dependent features of  $K(\tau, x)$  present at short times, and will therefore take a universal form depending only on the temperature, the mean level spacing and the typical slope of the single-particle energy levels at Fermi energy [24,20]. For (fully) chaotic systems we therefore need the random matrix theory result for this function. Changing for simplicity to the scaled variable  $t = \tau/\tau_H$ , using the definition  $K(t, x) = (1/\tau_H) K(\tau = \tau_H t, x)$  and scaling the parameter  $x$  according to the prescription given in [20], for chaotic systems without time reversal symmetry for instance ( $\beta = 2$ ) we can Fourier transform with respect to energy the parametric two-point correlation function obtained in [24]. We get

$$K_{rmt}(t, x) = \begin{cases} e^{-2\pi^2 x^2 t} \sinh(2\pi^2 x^2 t^2) / 2\pi^2 x^2 t & t \leq 1 \\ e^{-2\pi^2 x^2 t^2} \sinh(2\pi^2 x^2 t) / 2\pi^2 x^2 t & t > 1 \end{cases} \quad (60)$$

Inserting this in Eq.(59) the autocorrelation of the entropy may therefore be computed for temperatures well below  $E_c/2\pi^2$ .

## VII. DISCUSSION

It follows from Eqs.(12) and (13) that the three "intrinsic" energy scales that characterize the Fermi gas, namely  $E_F$ ,  $E_c$  and  $\delta$ , are determined by the number of fermions in the gas (taking into account degeneracies due to, e.g., spin), by their mass, and by the volume of the cavity (or, alternatively,  $\mu$ ,  $m$ , and  $V$  fix  $\bar{N}$ ,  $E_c$  and  $\delta$ ). The same is true for the adimensional shell-strength parameter  $g = E_c/\delta$ . They are independent of the precise shape of the system, and are therefore independent of the regular or chaotic nature of the single-particle dynamics.

	Metal particles	Nuclei
$N$	20 – 5000	25 – 250
$r = r_0 N^{1/3}$	0.5 – 3.5 nm	3.2 – 7 fm
$n = N/V$	30 electrons nm <sup>-3</sup>	0.17 nucleons fm <sup>-3</sup>
$k_F r$	10 – 67	11 – 25
$E_F$	35000 K	37 MeV
$E_c = \frac{\pi E_F}{k_F r}$	22000 – 3500 K	26.5 – 12.3 MeV
$\delta = \frac{2E_F}{3N}$	1200 – 5 K	1 – 0.1 MeV
$g = \frac{3\pi N}{2k_F r}$	20 – 760	27 – 125

**Table V:** Main features of metal particles and atomic nuclei as a function of particle number, ranging from 20 to 5000 and from 25 to 250, respectively.

It is useful to recall their typical magnitude as well as other relevant physical parameters for two important systems, metallic particles and atomic nuclei. Table V summarizes the main features. The number of particles is  $N$ , electrons or nucleons respectively. It typically ranges from 20 to several thousands in metal particles, and from 25 to 250 in nuclei. For definiteness, we take the window 20–5000 for metallic particles (although values up to 20000 can be reached experimentally [25]). The values indicated in the table are for these two windows, respectively. The radius  $r = r_0 N^{1/3}$  fixes the system size as a function of  $N$ . For metal particles  $r_0$  (which is sometimes denoted  $r_s$ ) ranges from 1 to 3Å. In the table we have used the typical value  $r_s = 2\text{Å}$ . For nuclei  $r_0 = 1.1$  fm.

Other relevant experimental systems, with much larger typical sizes, are the two-dimensional (2D) quantum dots. For instance, the electron gases contained in microscopic 2D cavities created in high mobility GaAs heterojunctions have a typical electronic density of  $n \approx 5 \times 10^{11}$  cm<sup>-2</sup> and Fermi energy  $E_F = 18$  meV (see, e.g., Ref. [26]). For typical quantum-dot sizes  $L \approx 0.1 - 5$  μm, the other characteristic energy scales vary in the range  $E_c \approx 6.4 - 0.128$  meV and  $\delta \approx 0.36 - 1.44 \times 10^{-4}$  meV. This gives an effective number of fermions in the last shell in the range  $g = 18 - 890$ .

The table illustrates the variations in the energy scales with the number of particles.  $E_c$  is comparable to  $E_F$  for small grains and nuclei. As the system grows, the three energy scales become however well separated, thus improving the applicability of the semiclassical methods.

As we have shown in the previous sections, the parameter  $g$  which, according to Table V, may take quite large values in real systems, plays an important role in setting the scale of the fluctuations of thermodynamic functions.

As summarized in Table II, it determines the relative value of the fluctuations in integrable systems as compared to chaotic ones for quantities like the energy or the response of the gas. This amplification factor is due to the special organization of periodic orbits in regular systems, which form one-parameter families, to be compared to the isolated character of periodic orbits for chaotic motion. Among the chaotic systems the variance is twice bigger in systems with time reversal symmetry.

It is instructive to compare the fluctuations of the energy and of the response function of the whole Fermi gas with the corresponding fluctuations of a single-particle energy level located in the neighborhood of the Fermi energy. When an external parameter is varied, the fluctuations of the energy of a single-particle level located at  $E \approx E_F$  may be computed from the fluctuations of the Fermi energy of a system with a fixed number of particles  $N$ . The number of particles is related to the Fermi energy through the spectral counting function,  $N = \mathcal{N}(E_F)$ . Writing  $E_F = \overline{E}_F + \tilde{E}_F$  and also splitting  $\mathcal{N}$  into its smooth and oscillatory parts, expanding when appropriate by assuming  $\tilde{E}_F \ll \overline{E}_F$ , and ignoring second order terms in the fluctuations we arrive at  $N = \overline{\mathcal{N}}(\overline{E}_F) + \overline{\rho}(\overline{E}_F)\tilde{E}_F + \tilde{\mathcal{N}}(\overline{E}_F)$ . But  $\overline{E}_F$  is precisely defined in order to satisfy  $\overline{\mathcal{N}}(\overline{E}_F) = N$ . The fluctuations of a single-particle level, estimated by  $\tilde{E}_{sp} \approx \tilde{E}_F$ , are therefore

$$\tilde{E}_{sp} = -\tilde{\mathcal{N}}(\overline{E}_F) \delta \quad (61)$$

with the variance

$$\langle \tilde{E}_{sp}^2 \rangle = \langle \tilde{\mathcal{N}}^2 \rangle \delta^2 . \quad (62)$$

This relation allows, together with the variance of the particle number summarized in Table II, to connect the energy fluctuations of the gas with those of the single particle levels. To leading order in  $g$  we get

$$\langle \tilde{U}^2 \rangle = \begin{cases} \frac{1}{12\pi^2} g^2 \langle \tilde{E}_{sp}^2 \rangle & \text{integrable ,} \\ \frac{1}{8\pi^2} \frac{g^2}{\log g} \langle \tilde{E}_{sp}^2 \rangle & \text{chaotic .} \end{cases} \quad (63)$$

To establish a similar connexion for the response function we must first determine the local fluctuations of the response of the single-particle energy levels

$$R_{sp} = \frac{\partial E_j}{\partial x} , \quad (64)$$

where  $E_j \approx E_F$ . It was shown in Ref. [20] that in chaotic systems the variance of  $R_{sp}$  (with respect to a mean which is subtracted) is

$$\langle \tilde{R}_{sp}^2 \rangle = \frac{2\alpha}{\beta\tau_H} = \frac{2\alpha}{\beta\tau_{min}} \frac{1}{g} , \quad (65)$$

where  $\alpha$  was defined in Eq.(33). A similar computation for integrable systems gives, using the corresponding relation in Eq.(33)

$$\langle \tilde{R}_{sp}^2 \rangle = \omega . \quad (66)$$

Using these relations together with the results for the variance of the response of the gas  $\langle \tilde{R}^2 \rangle$  from Table II we find

$$\langle \tilde{R}^2 \rangle = \frac{1}{2\pi^2} g \langle \tilde{R}_{sp}^2 \rangle \quad (67)$$

for both regular and chaotic dynamics.

The global picture emerging from these relations is quite instructive. Contrary to naive expectations, Eq.(62) shows that the typical fluctuations of a single-particle level located at  $E_F$  are not of order  $\delta$ , but are "amplified" by the fluctuations of the particle number. Since the latter are larger in integrable systems compared to chaotic ones (by a relative factor  $\sqrt{g/\log g}$ ), then  $\sqrt{\langle \tilde{E}_{sp}^2 \rangle_{int} / \langle \tilde{E}_{sp}^2 \rangle_{ch}} \propto \sqrt{g/\log g}$ . Eq.(63) shows, moreover, that the fluctuations of the energy of the gas are, in turn, much larger than the local variations. Similar considerations hold for the response. We see from Eq.(67) that the typical response of the gas,  $R_{typ} = \sqrt{\langle \tilde{R}^2 \rangle}$ , is  $\sqrt{g}$  times greater than that of the single-particle levels located at  $E_F$ , irrespective of the integrable or chaotic nature of the dynamics. One should however keep

in mind that  $\langle \tilde{R}_{sp}^2 \rangle$  is bigger in integrable systems with respect to chaotic ones by a factor of order  $g$ , and therefore the overall fluctuations of the response of the gas are more important if the dynamics is integrable. When computed in the particular case of the persistent currents in mesoscopic rings,  $I = -c \partial\Omega/\partial\phi$ , where the external parameter  $x$  is now the magnetic flux threading the ring, the formula  $\langle \tilde{R}^2 \rangle = \alpha/(\pi^2\tau_{min})$  in Table II valid for chaotic systems gives for the typical current  $I_{typ} = \sqrt{\langle \tilde{I}^2 \rangle} = (\sqrt{2}c/\pi)E_c/\phi_0$  (where  $c$  is the speed of light and  $\phi_0$  the flux quantum), in agreement with the result obtained in [27] using a Green's-function approach, and with the  $\sqrt{g}$  amplification obtained for integrable systems (see also [28]).

All this results clearly show the close connexions existing between the fluctuations of the gas and the parameter  $g$ . Remember that  $g = E_c/\delta$  is the number of fermions contained in the last shell, i.e. in a window of size  $E_c$  below the Fermi energy. This number of particles has to be compared with the total number of fermions  $N = (2/d)E_F/\delta$  (in  $d$  dimensions). Eqs. (63) and (67) show that neither the total number of particles, nor an individual single-particle level (located at  $E_F$ ), are responsible for the fluctuations of the gas, but rather the intermediate number  $g$ , with typically  $1 \ll g \ll N$ . The quantum fluctuations of the gas therefore originate from the contributions of the  $g$  particles located in the last shell, as already pointed out in Ref. [11]. However, the way these particles contribute to the fluctuations depend on the quantity considered. Eq. (63) shows that they contribute "coherently" in the case of the total ground-state energy, since  $U_{typ} = \sqrt{\langle \tilde{U}^2 \rangle}$  is proportional to  $g$  (ignoring the  $\log g$  denominator in the chaotic case). In contrast, their contributions to the response add up "incoherently" (as in a random walk), as shown by Eq. (67). Physically, this may be interpreted as the independence of the slopes  $\partial E_j/\partial x$  of the last  $g$  single-particle levels.

The situation is more subtle for quantities like the entropy. As was shown in section IV B, the temperature dependence of the variance for  $k_B T \ll \delta/2\pi^2$  is unique, independent of the nature of the single-particle dynamics (and given by Eq. (39)). However, at higher temperatures differences are observed. The maximum of the typical value of the entropy fluctuations,  $S_{typ} = \sqrt{\langle \tilde{S}^2 \rangle}$ , is of order  $k_B$  for chaotic systems, and it is reached at  $2\pi^2 k_B T \approx \delta$ , whereas for integrable systems  $S_{typ}$  grows up to values  $\propto g k_B$ . The maximum value in integrable systems is reached at temperatures  $2\pi^2 k_B T \approx E_c$ .

There are several distinct applications of the present results. Among them, we mentioned the study of the electronic contribution to the mechanical force in experiments where metallic nanocontacts are pulled [29], and the fluctuations of the energy of nuclei as a function of the number of nucleons. Progress made in both directions will be published elsewhere. In a related work, the distribution of the energy of a Fermi gas whose single-particle energy levels are given by the imaginary part of the complex zeros of the Riemann zeta function was recently investigated [30]. This fictitious fermionic system was named "the Riemannium". Aside its mathematical interest, it serves as an explicit and important test of our results relating the probability distribution of thermodynamic functions to periodic orbit theory. This is because there exist strong connexions between the quantum theory of chaotic systems and the complex zeros of the Riemann zeta function interpreted as spectral eigenvalues. A high precision agreement was found between the numerical results and the moments of the probability distribution of  $\tilde{\Omega}$  computed from the results of Section V A for the Riemannium.

## VIII. CONCLUDING REMARKS

Our results illustrate the strong connexions and deep relationships that exist between, on the one hand, the thermodynamic quantum fluctuations of confined Fermi gases and, on the other, the statistical theories of level fluctuations and periodic orbit theory.

The regular or chaotic nature of the single-particle motion imprints the single-particle spectrum in two different ways. The first one occurs at the scale of the mean level spacing  $\delta$ , and produces different (but universal) statistical fluctuations. The second acts on a much larger scale  $E_c$ , set by the inverse of the time of flight across the system. A bunching of the single-particle levels produced by the short periodic orbits is observed on this scale, whose intensity depends on the regular or chaotic nature of the motion.

The main theme of our investigations has been to determine how these two features of the single-particle spectrum influence the probability distribution of the quantum fluctuations of the different thermodynamic functions of the gas, and to establish their temperature dependence. We find a rich variety of phenomena and of different regimes. In some cases the thermodynamic quantum fluctuations directly reflect the universality of the single-particle spectrum on the scale  $\delta$ . Their corresponding probability distributions are universal functions, whose shape depends on the quantity and temperature considered, and on the regular or chaotic nature of the dynamics, but not on the precise shape or other specific properties of the system. In other cases, the fluctuations are, in contrast, totally determined

by the long-range modulations of the single-particle spectrum on scales  $E_c$ . They are therefore insensitive to the universality present on the scale  $\delta$ . For some thermodynamic quantities, this type of fluctuations are dominant even at zero temperature. The shape of the distributions is, in this case, system-dependent and therefore non-universal. The moments may be computed from the short periodic orbits of the single-particle dynamics. At temperatures of order  $E_c$  or higher, all the thermodynamic fluctuations, even those dominated at low temperatures by the universal features of the single-particle spectrum, fall in this second class. In all cases and for the different regimes, we have shown how the probability distributions can be explicitly computed in each case.

The variance of the thermodynamic functions has also been investigated using a simple approximation, that takes only into account the regular or chaotic nature of the single-particle dynamics and the time of flight across the system. It has the advantage of providing a good qualitative description for the different thermodynamic quantities as a function of temperature, number of particles, etc, while requiring a minimum amount of information about the system. Although more accurate descriptions can be made if more information is available, this approximation is clearly of interest in experiments where the parameters controlling the system, like its shape, are not well known.

A closely related problem is the motion of quasiparticles in potentials with bulk disorder. This case has been extensively treated in condensed matter physics in particular as a model for the electronic properties of metals and semiconductors. Compared to the ballistic motion considered here, the disorder introduces a new scale, the elastic mean free path  $\ell_e$  between impurities. When  $\ell_e$  is much smaller than the system size  $L$  (and  $L$  is much smaller than the localization length), the single-particle motion across the system is diffusive. The corresponding energy scale is the Thouless energy,  $E_c = \hbar D/L^2$ , with  $D$  the diffusion coefficient. Similarly to the influence of the (short) periodic orbits in the ballistic case, the diffusive motion produces long-range correlations in the single-particle spectrum [31]. However, the nature of the correlations are different in both cases. Therefore, the statistics of the quantum thermodynamic fluctuations that are dominated by the long range correlations are going to be different. An analogous study for diffusive systems to the one made here in the ballistic case is therefore necessary. In contrast, it has been shown that the local fluctuations of the single-particle levels on a scale  $\delta$  are, in the metallic regime of disordered systems, also described by random matrix theory [32]. Therefore, our results concerning the quantum fluctuations of thermodynamic quantities in the universal regime apply also to disordered systems.

The quantum fluctuations considered may be compared to other fluctuations, the thermal ones. Although the latter are inherent to any thermodynamical treatment, their physical origin and their experimental manifestation is very different from that of the quantum fluctuations here considered.

Many experiments have verified the validity and accuracy of the physical picture obtained from mean-field, single-particle approximations to many-body systems. However the nature of the modifications induced by the (residual) interactions in the probability distribution of the thermodynamic fluctuations remains an open problem.

**Acknowledgements:** we are in debt with C. Schmit who kindly bring us the numerical spectrum of the Sinai cavity.

- 
- [1] A. Bohr and B. R. Mottelson, *Nuclear Structure*, Benjamin, Reading, MS, 1969, Vol.I.
  - [2] M. Brack, *Rev. Mod. Phys.* **65** (1993) 677.
  - [3] R. Balian and C. Bloch, *Ann. Phys. (N.Y.)* **69** (1972) 76.
  - [4] V. M. Strutinsky and A. G. Magner, *Sov. J. Part. Nucl.* **7** (1976) 138.
  - [5] O. Bohigas, M.-J. Giannoni, and C. Schmit, *Phys. Rev. Lett.* **52** (1984) 1.
  - [6] M. V. Berry and M. Tabor, *Proc. R. Soc. Lond. A* **356** (1977) 375.
  - [7] K. Efetov, *Supersymmetry in Disordered and Chaos*, Cambridge University Press, Cambridge, 1997.
  - [8] Y. Imry, *Introduction to Mesoscopic Physics*, Oxford University Press, New York, 1997, and references therein.
  - [9] K. Richter, D. Ullmo and R. Jalabert, *Phys. Rep.* **276** (1996) 1.
  - [10] L. Landau and E. M. Lifchitz, *Physique Statistique*, Éditions Mir, Moscou, 1988.
  - [11] M. Brack, J. Damgaard, A. S. Jensen, H. C. Pauli, V. M. Strutinsky, and C. Y. Wong, *Rev. Mod. Phys.* **44** (1972) 320.
  - [12] M. C. Gutzwiller, *Chaos in Classical and Quantum Mechanics*, Springer, New York, 1990.
  - [13] M. V. Berry and M. Tabor, *J. Phys. A* **10** (1977) 371.
  - [14] O. Agam, *J. Phys. I France* **4** (1994) 697.
  - [15] J. T. Edwards and D. J. Thouless, *J. Phys. C* **5** (1972) 807.
  - [16] M. V. Berry, *Proc. Roy. Soc. Lond. A* **400** (1985) 229.
  - [17] G. Montambaux in *Quantum Fluctuations* (S. Reynaud, E. Giacobino and J. Zinn-Justin, Eds.), Les Houches Session

- LXIII, p.387, North Holland, Amsterdam, 1997.
- [18] O. Bohigas in *Chaos and Quantum Physics* (M.-J. Gianonni, A. Voros and J. Zinn-Justin, Eds.), Les Houches Session LII, p.87, North Holland, Amsterdam, 1991.
  - [19] J. Goldberg, U. Smilansky, M. V. Berry, W. Schweizer, G. Wunner and G. Zeller, *Nonlinearity* **4** (1991) 1.
  - [20] P. Leboeuf and M. Sieber, *Phys. Rev. E* **60** (1999) 3969.
  - [21] P. Leboeuf and A. Monastra, *Phys. Rev. B* **62** (2000) 12617.
  - [22] J. Hannay and A. M. Ozorio de Almeida, *J. Phys. A* **17** (1984) 3429.
  - [23] R. Aurich, A. Bäcker and F. Steiner, *Int. J. Mod. Phys. B* **11** (1997) 805.
  - [24] B. D. Simons and B. L. Altshuler, *Phys. Rev. B* **48** (1993) 5422; *Phys. Rev. Lett.* **70** (1993) 4063.
  - [25] T. P. Martin, T. Bergmann, H. Göhlich and T. Lange, *Zeit Phys.* **D19** (1991) 25.
  - [26] C. W. Beenakker and H. van Houten in *Solid State Physics* (H. Ehrenreich and D. Turnbull, Eds.) **44**, 1, Academic, New York, 1991; L. L. Sohn, L. P. Kouwenhoven and G. Schon, *Mesoscopic Electron Transport in Semiconductor Nanostructures*, Kluwer Academic, Boston, 1997.
  - [27] H. Cheung, E. Riedel and Y. Gefen, *Phys. Rev. Lett.* **62** (1989) 587.
  - [28] A. Atland and Y. Gefen, *Phys. Rev. B* **51** (1995) 10671.
  - [29] G. Rubio, N. Agraït and S. Vieira, *Phys. Rev. Lett.* **76** (1996) 2302.
  - [30] P. Leboeuf, A. G. Monastra and O. Bohigas, *Reg. Chaot. Dyn.* **6** (2001) 205.
  - [31] B. L. Altshuler and B. I. Shklovskii, *Zh. Eksp. Teor. Fiz.* **91** (1986) 220 [*Sov. Phys. JETP* **64** (1986) 127].
  - [32] K. Efetov, *Adv. Phys.* **32** (1983) 53.